DE LA RECHERCHE À L'INDUSTRIE

www.cea.fr

ACCELERATOR TESTING OF MATERIALS

Dr. Celine Cabet

CEA, DEN, DMN
Service de Recherches de Métallurgie Physique
JANNUS laboratory

+33 1 69 08 16 15 celine.cabet@cea.fr

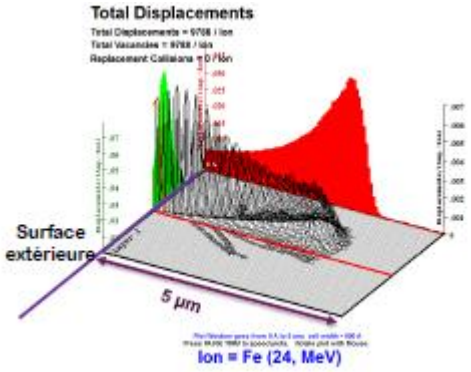

Outline

1. Background on ion-irradiation of materials

Examples - use of ion-beams for nuclear material studies

2. Formation of extended radiation-defects in UO_2
3. Role of irradiation in oxidation of Zr-alloys
4. Precipitation in model ferritic alloys
   dose rate effect

5. Conclusion

1. Effects of neutron irradiation in materials

Ballistic damage

Change in the **structure**

Nuclear reactions

Change in **composition**

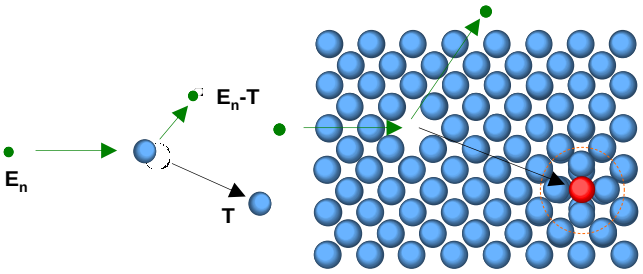

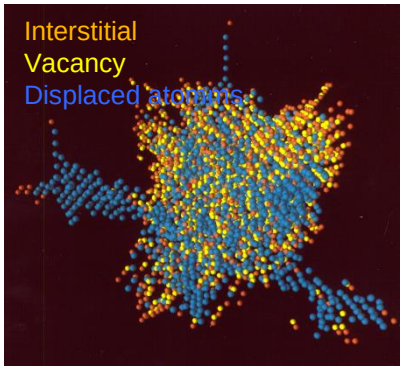

- **Production of He and H by (n, α) and (n, p) reactions**
- **Transmutation products**
- **Fission products**

Kinetic energy transfer *

Defect formation in the crystalline lattice: vacancies and interstitials

Displacement cascade : 1 neutron → 300 defects

- Change in **dimension**
- Changes in thermo-mechanical **properties**

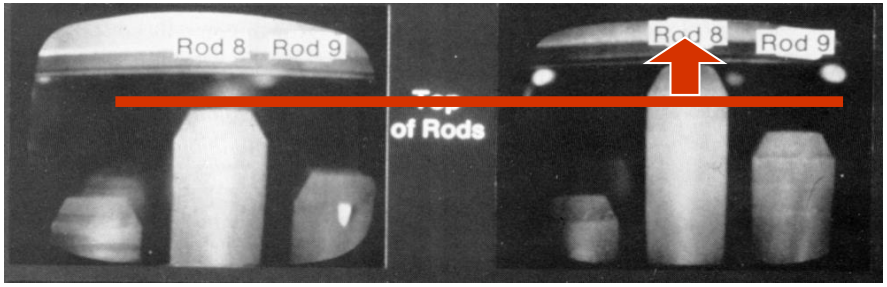

PWR fuel cladding

1. Effect of ion irradiation in materials - use of SRIM

Ballistic damage

Epiméthée, Fe 2 MeV (self ion)

FeCr 45.5%, 700°C, 3.43 10^{15} Fe^{3+}/cm^2

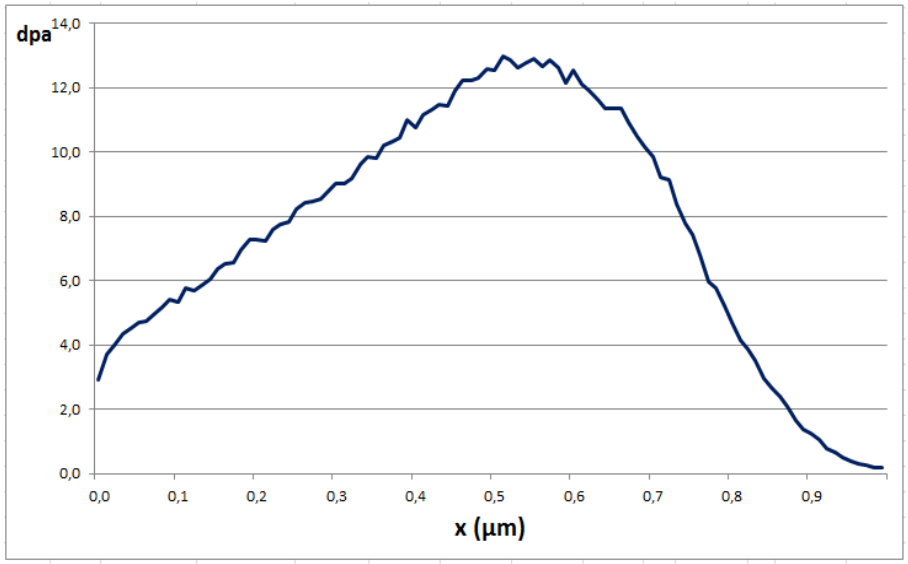

Irradiation profile from SRIM (KP damage mode)

Gas implantation

Epiméthée, He 2 MeV

FeCr 10%, RT, 1.2 10^{17} He^{+}/cm^2

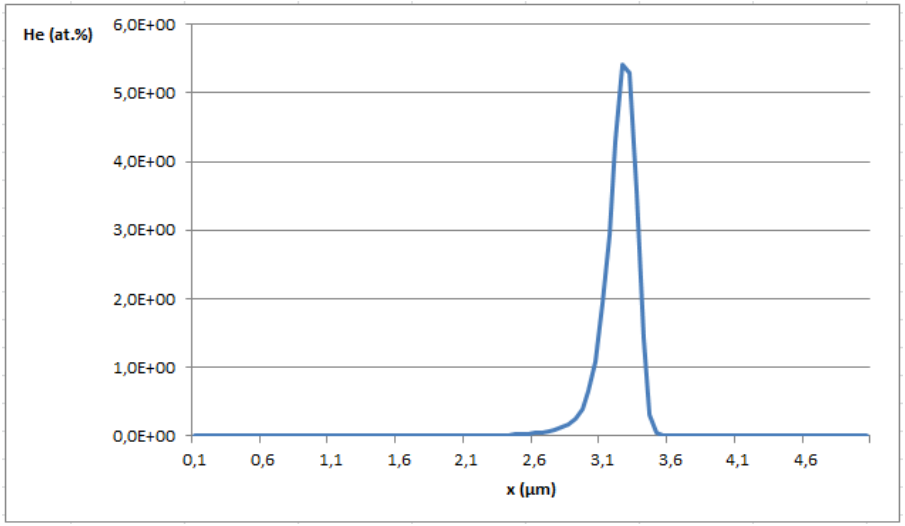

Irradiation profile from SRIM (KP damage mode)

1. Selection of the zone of interest

Irradiation profile for Fe 2 MeV in 316 SS at a depth of 300 nm:
- **Damage rate**: ≈**2.8 10^{-3} dpa/s**
- **Dose**: ≈100 dpa (1 day)

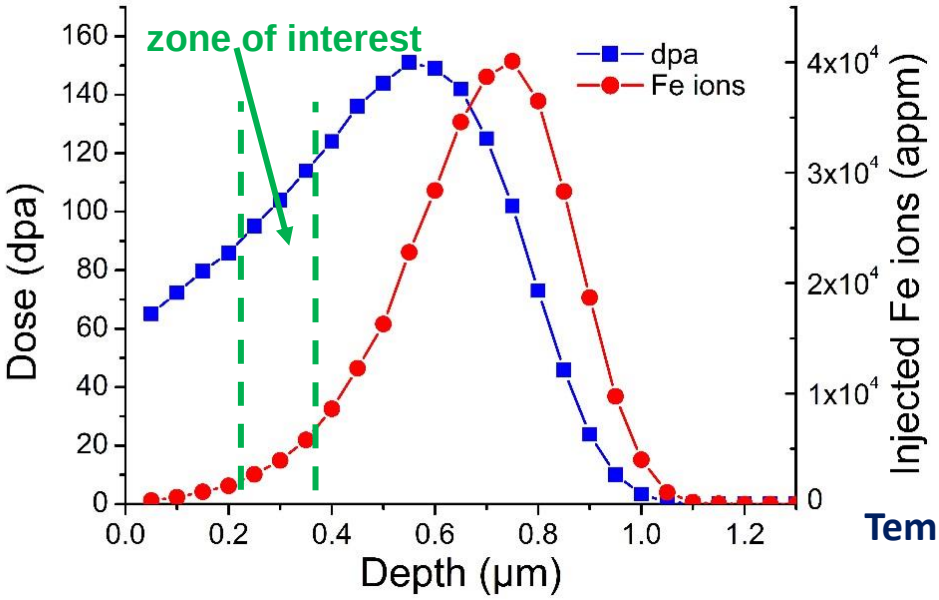

Temperature: 300°C

near surface

Advantages
- Low ion implantation

Drawbacks
- Possible oxidation and carbon deposit
- Surface is a sink

medium depth

Advantages
- Low ion implantation
- Accurate dose evaluation

Drawbacks
- Longer irradiation time

>0.5µm

Advantages
- High dose

Drawbacks
- Ion implantation
- Uncertainty on the dose (KP vs full cascade damage)

1. Dual ion-beam irradiation

Ballistic damage

Epémithée, Fe 10 MeV
2 10^{12} $cm^{-2}.s^{-1}$

Gas implantation

Pandore, He 1.1 MeV
2.3 10^{11} $cm^{-2}.s^{-1}$
with use of degraders

316SS

Irradiation profiles in 316 from SRIM (KP damage mode) after 6 hours at 650 nm:
- **Dose: ≈10 dpa (1.2 10^{17} /cm^2)**
- **15 appm/dpa**

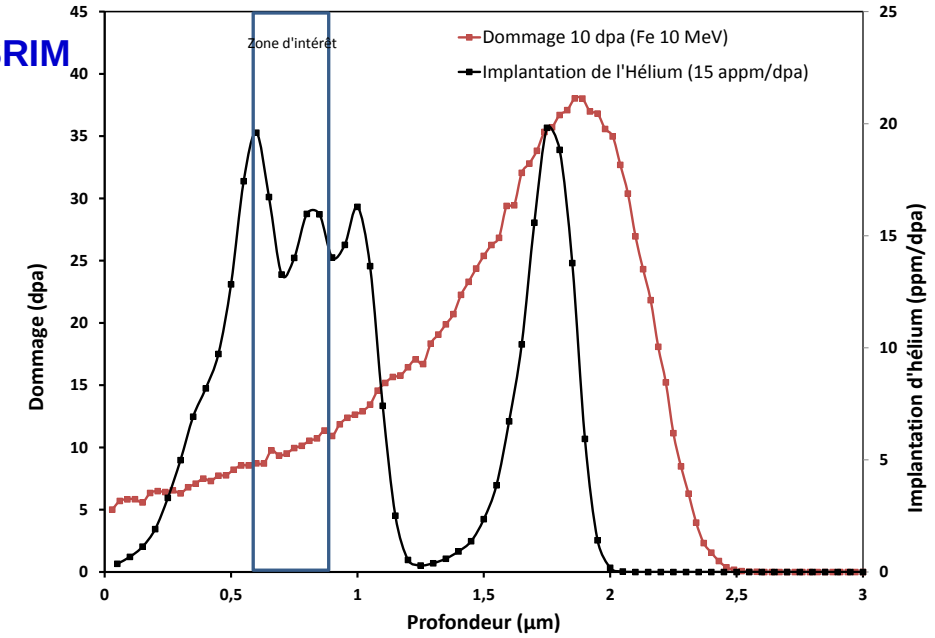

Sequential gas injection and heavy ion bombardment is not equivalent to simultaneous irradiation

Brimhall and Simonen (1977)
Lévy, Gilbon and Rivera (1985)

1. Ion accelerators facility for material testing
JANNuS-Saclay

Heavy ion damage
Hydrogen implantation

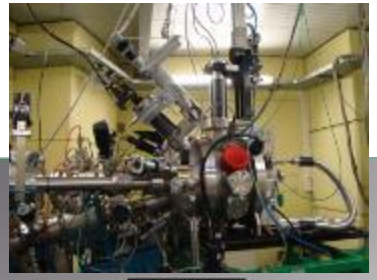

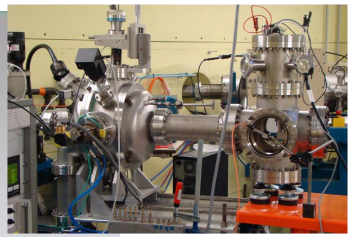

Heavy ion damage
Helium and hydrogen implantation

Helium and hydrogen implantation

1. JANNuS-Saclay: 3 MV Pelletron Épiméthée

➢ **Accelerator: 3 MV Pelletron NEC (National Electrostatics Corporation) with a ECR (Electron Cyclotron Resonance) source from Pantechnik**

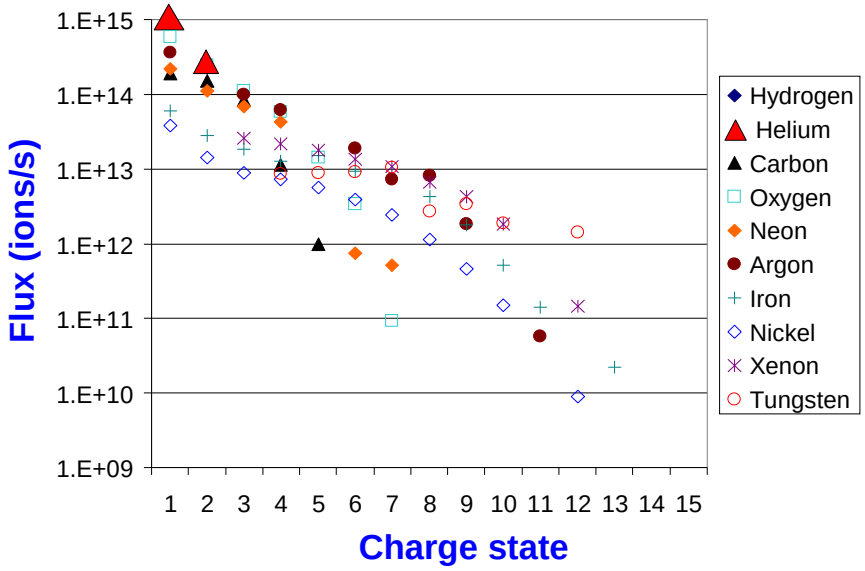

⇨ **Positive multi-charged ions**
1 < m < 209
400 keV < E < 40 MeV

Ballistic damage with Fe (~10 dpa/h)

1. JANNuS-Saclay: 2 MV Tandem Japet and 2.5 MV Pelletron Pandore

JAPET 2 MV Tandem with Source of Negative Ions by Cesium Sputtering (SNICS II)

⇨ **Negative single-charged ions are converted into positive multi-charged ions through the stripper**

PANDORE 2.5 MV Pelletron with Radio Frequence source

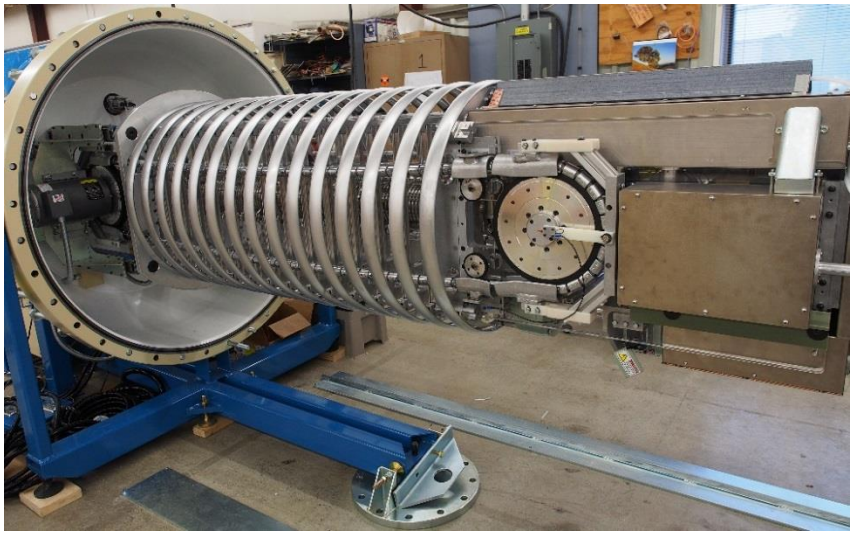

⇨ **Single-charged gasses: H, He, D, N, Ar**

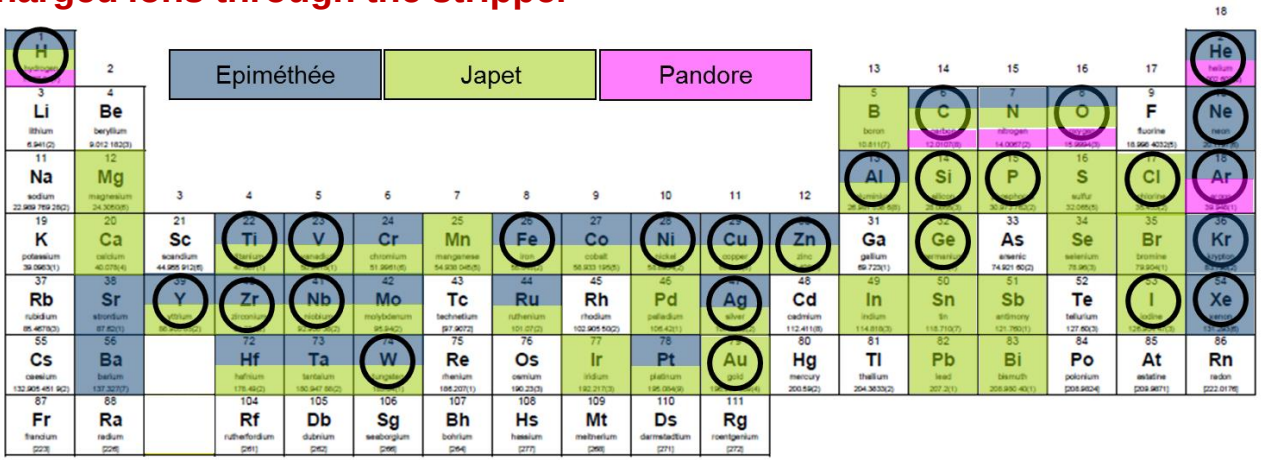

1. JANNuS-Saclay: Irradiation chambers

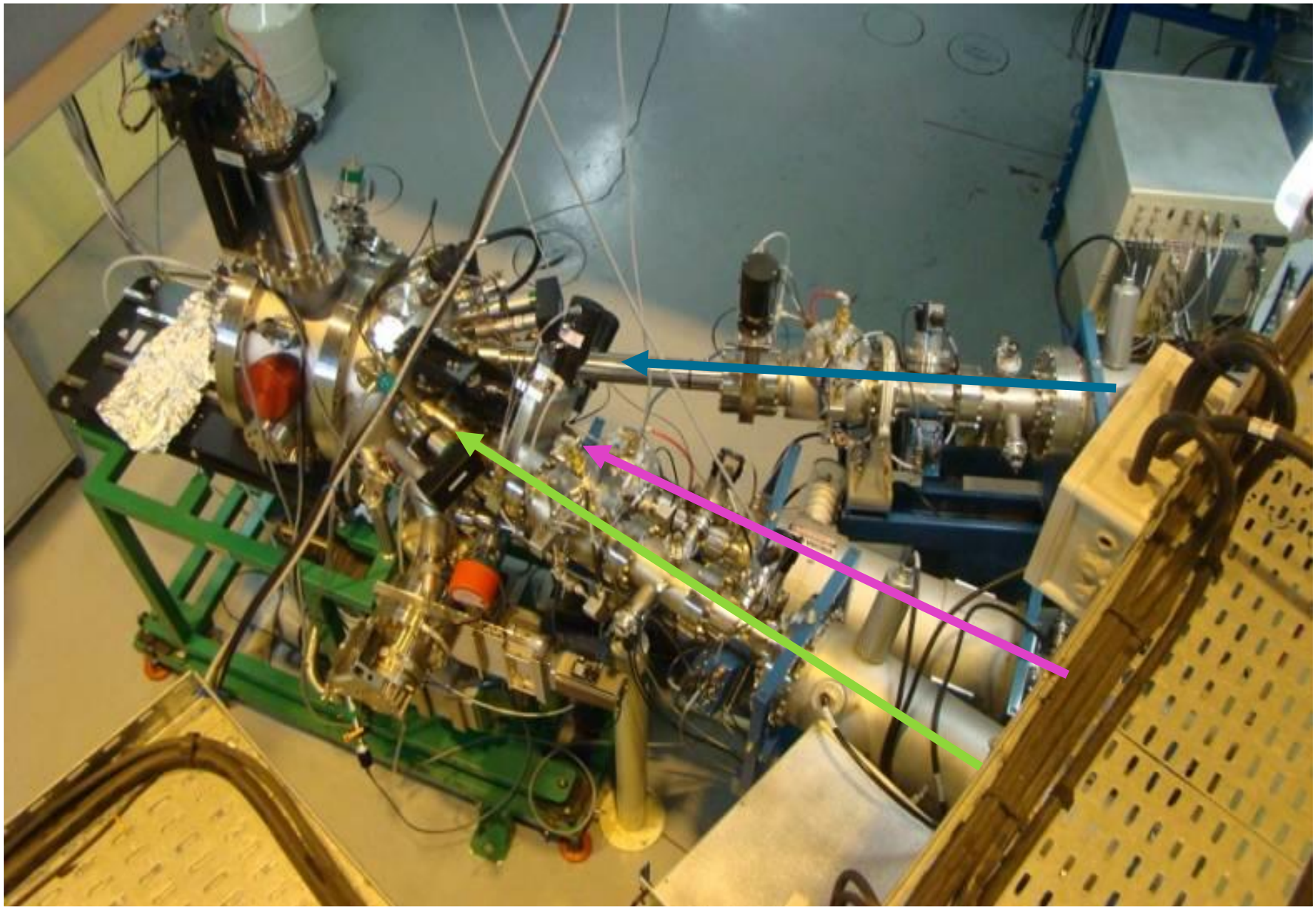

1. The *in situ* dual ion beam TEM at CSNSM : JANNuS-Orsay facility

Ion Beam Analysis
RBS, RBS/C, ERDA,
PIXE, *µPIXE, PIGE*

implantation / irradiation
LN_2 –> 1000°C

ARAMIS
2MV Tandem - VdG
0.5 – 11 MeV *
10 nA – 10µA

> 40 elements
* limited to 1 MeV per charge state inside the TEM

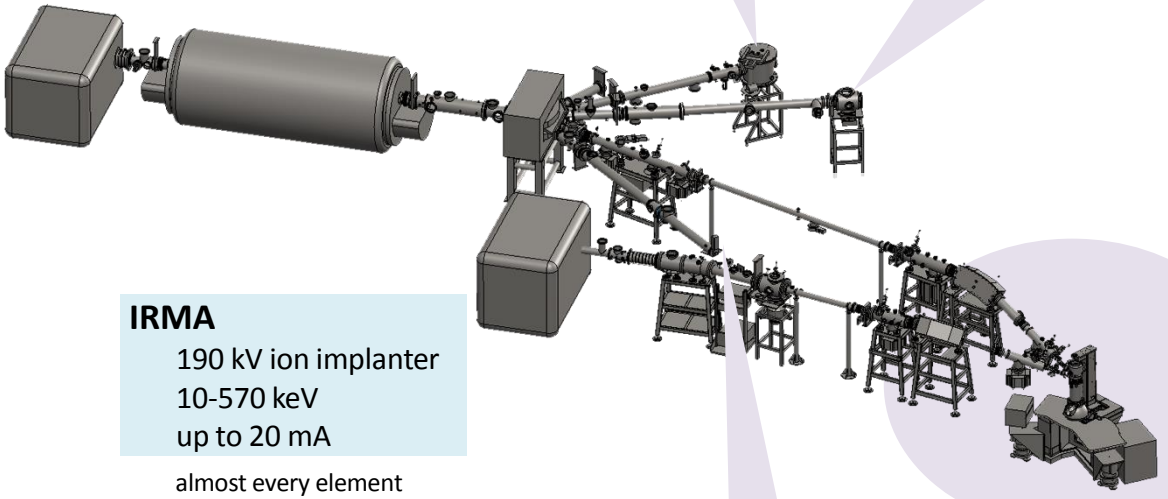

IRMA
190 kV ion implanter
10-570 keV
up to 20 mA

almost every element

in situ RBS/C
and implantation
LN_2 –> 600°C

TRANSMISSION ELECTRON MICROSCOPE
200 kV *FEI Tecnai G2 F20 Twin*
Resolution: 0.25 nm
Magnification range: 70-700 000

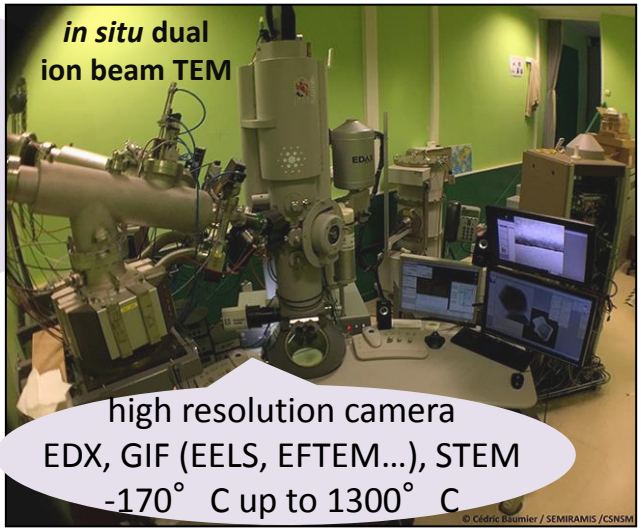

Formation of extended radiation-defects in UO_2

2. Ageing of nuclear fuel - background

C. Onofri et al.

UO_2 is the base of PWR fuel

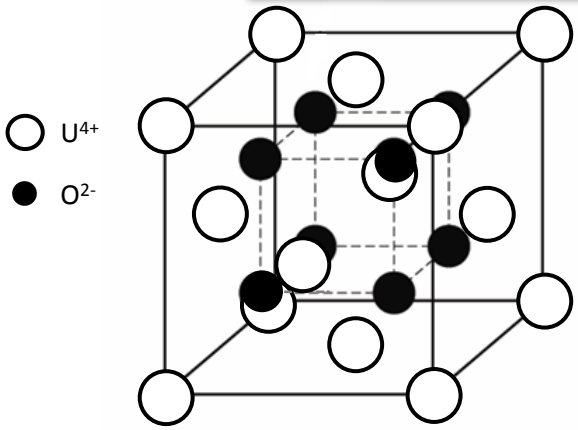

UO_2 crystalline structure: fluorite (cubic)

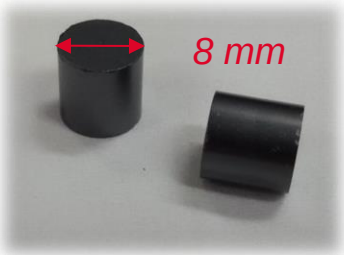

Sintered UO_2 pellets

Heavy nuclei fission

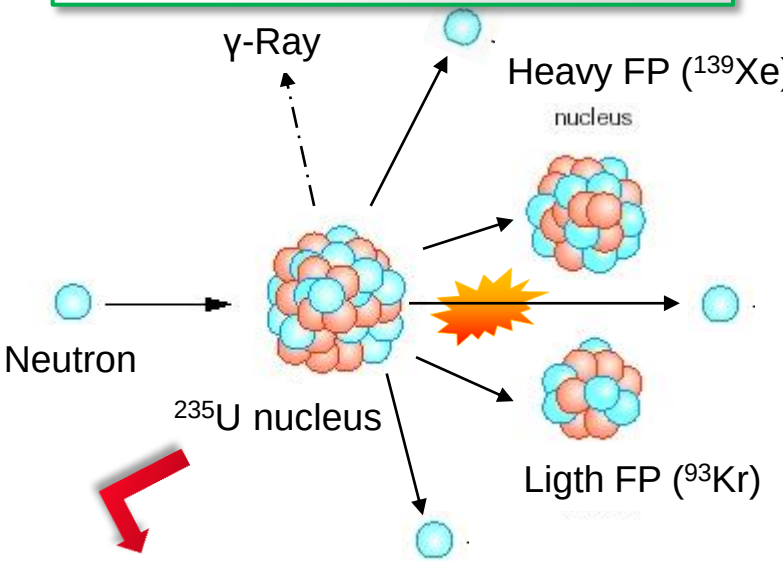

Energy from fission is ~ 200 MeV
~80 % is transmitted to FP as kinetic energy

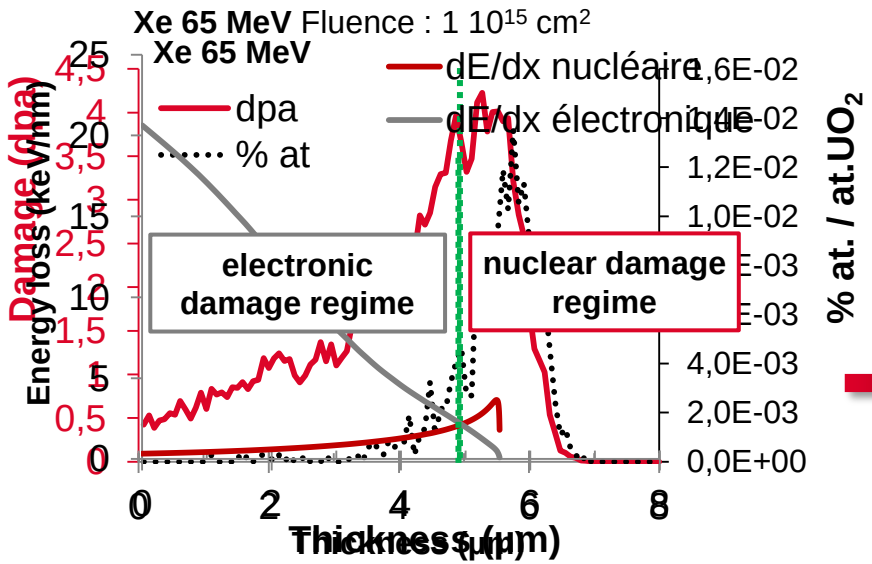

Changes in structure and physico-chemistry
(radiation induced defects, FP doping…)

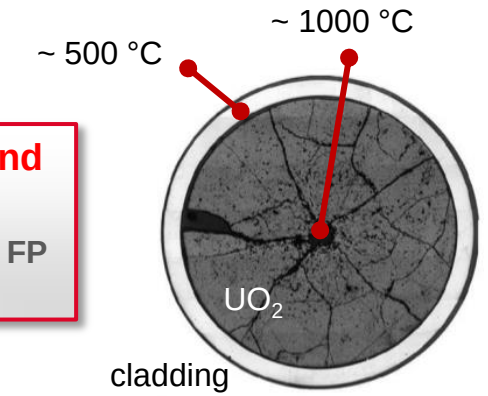

[1] T. Sonoda *et al.*, *Nucl. Instr. and Meth.* B 191 (2002) 622-628

2. Ageing of nuclear fuel - background

C. Onofri, C. Sabathier, M. Legros et al.

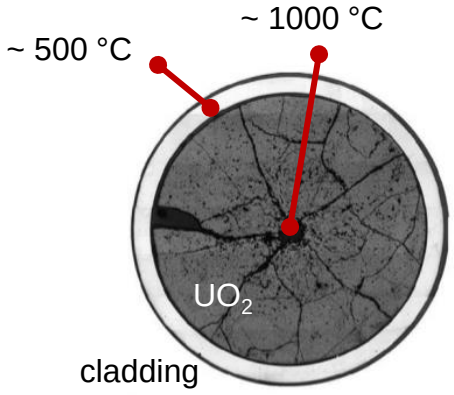

Load
Temperature
Radiation damage
Fuel/clad interaction…

Changes in structure and physico-chemistry
(radiation induced defects, FP doping…)

Complex and interrelated features

Specific study on the extended defects formation using Xe- and Kr-ion irradiation

Microstructure of in-pile irradiated UO_2

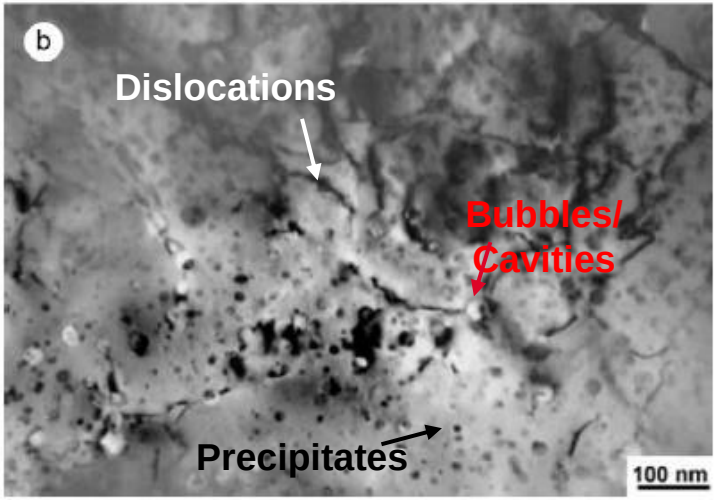

UO_2 fuel irradiated in reactor at ~450°C for 5 cycles (55 MWj/kgU) [2]

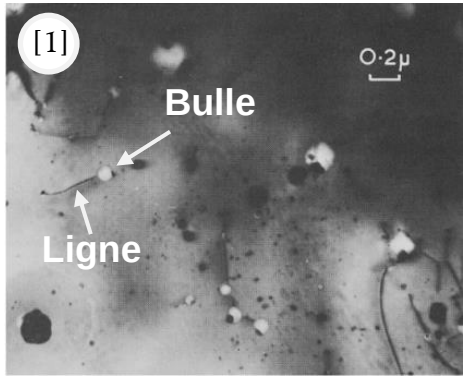

Neutron irradiated UO_2 annealed at 1500 °C

[1] A. D. Whapham. *Nuclear Applications* 2 (1966) 123
[2] T. Sonoda *et al.*, *Nucl. Instr. and Meth*. B 191 (2002) 622-628

2. Evolution of extended defects in UO_2 under Xe irradiation

C. Onofri, C. Sabathier, M. Legros et al.

In situ TEM at JANNuS-Orsay

390 keV Xe at -180 °C

0.06 | 0.18 | 0.6 | 1.8 Damage (dpa)

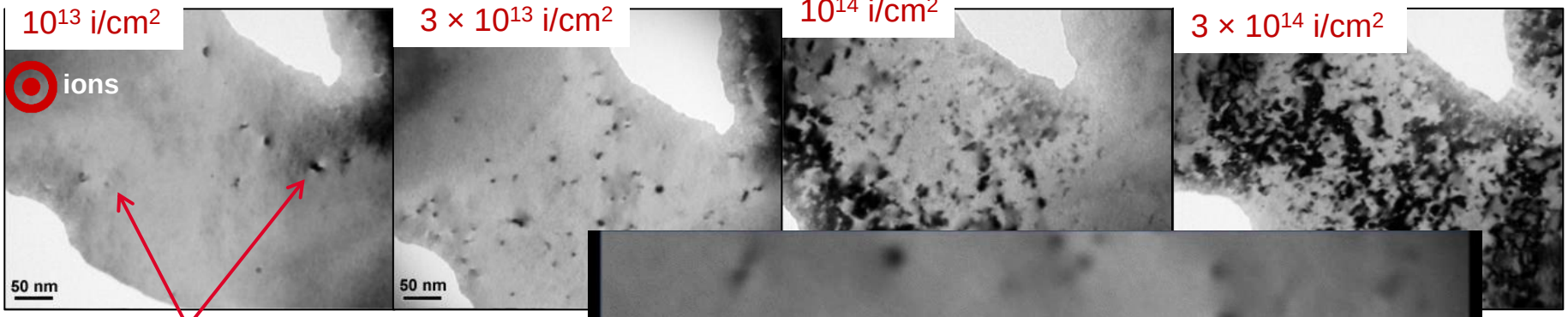

Defect clusters → **Future dislocation loops**

Small lo

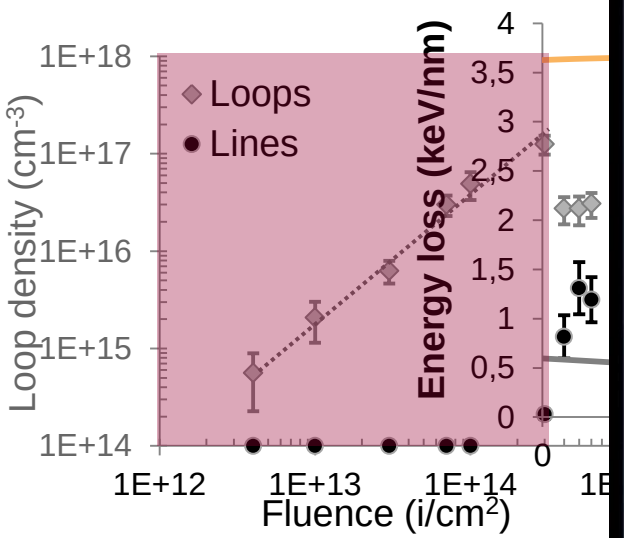

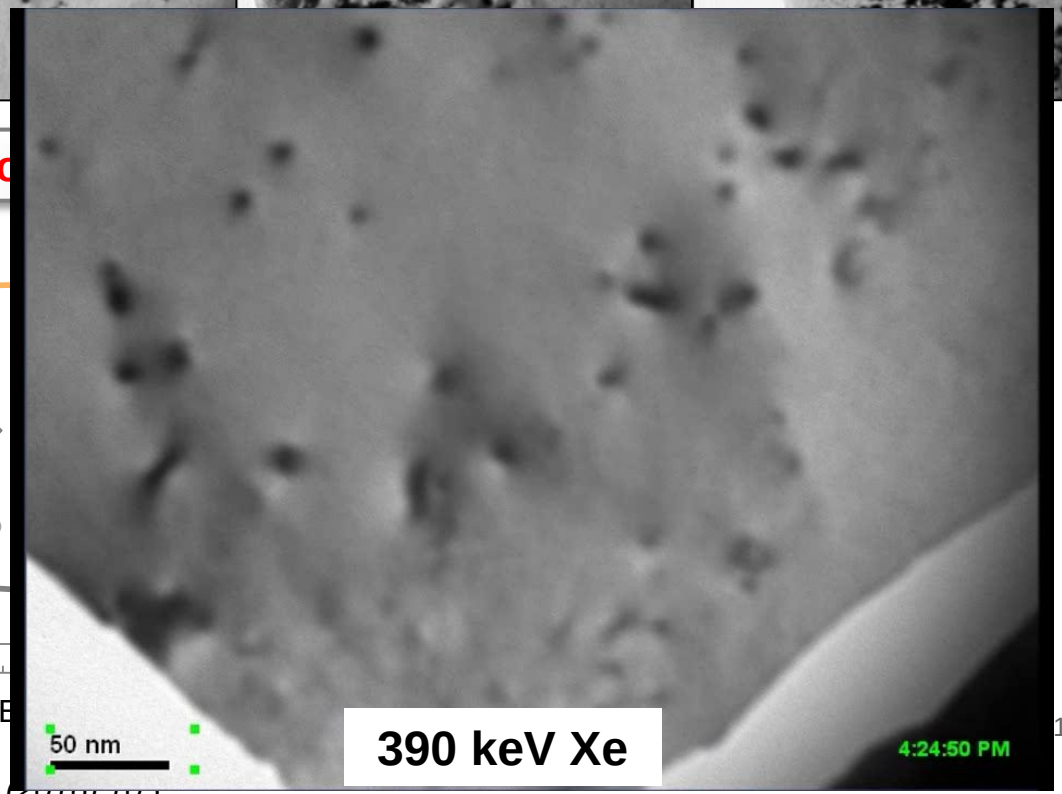

C. Onofri, C. Sabathier, C. Baumier et al., JNM 482 (2016) 165

2. Evolution of extended defects in UO_2 under Xe irradiation

C. Onofri, C. Sabathier, M. Legros et al.

In situ TEM at JANNuS-Orsay

390 keV Xe at -180 °C

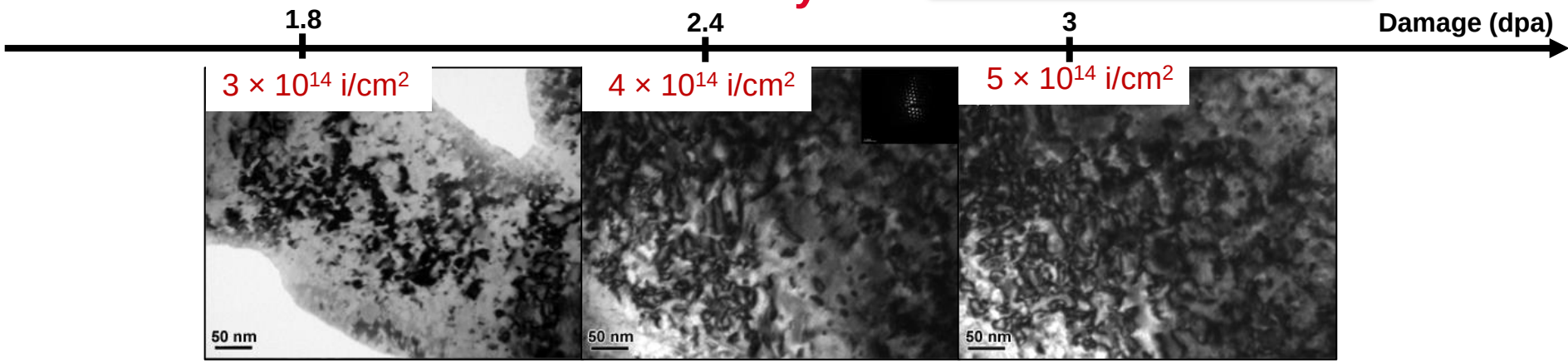

Loops overlapping for geometric reasons
➡ Transformation into lines

Steady state equilibrium
➡ Lines and small loops (< 10 nm)

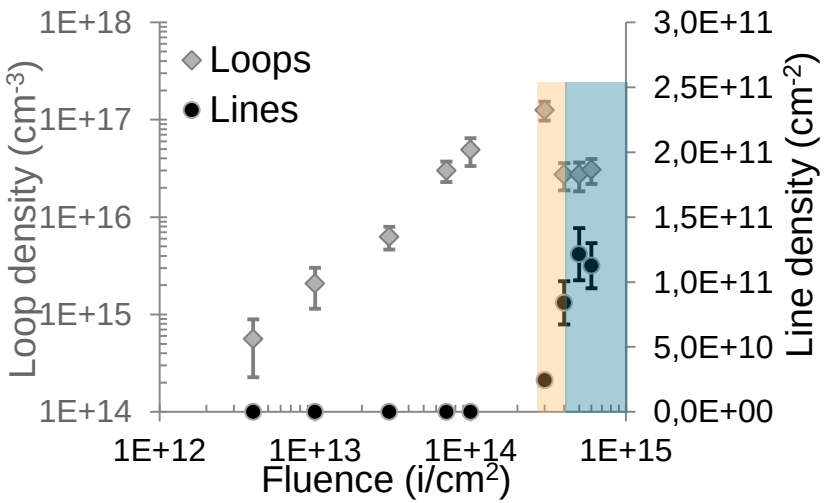

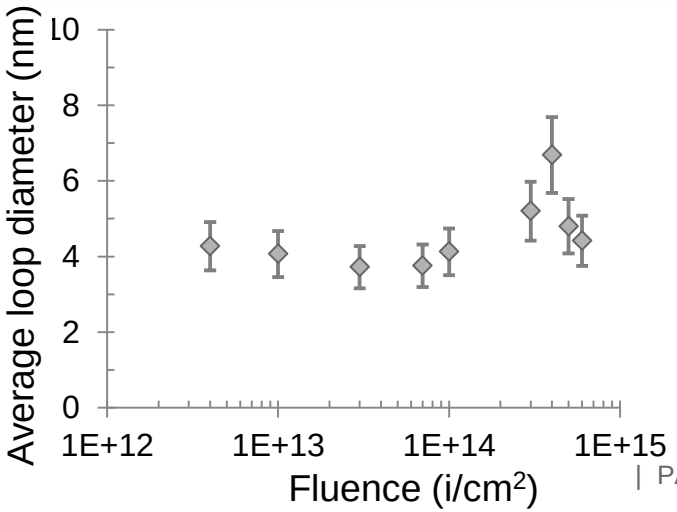

C. Onofri, C. Sabathier, C. Baumier et al., JNM 482 (2016) 105

2. Evolution of extended defects in UO_2 under Xe irradiation

C. Onofri, C. Sabathier, S. Miro et al.

4 MeV Kr at -160 °C

In situ Raman at JANNuS-Saclay

- No evolution
- Shrinking of defects band
- Decrease of T_{2g} intensity – *Loss of symmetry*
- Increase of defects band intensity – *Production of irradiation defects*

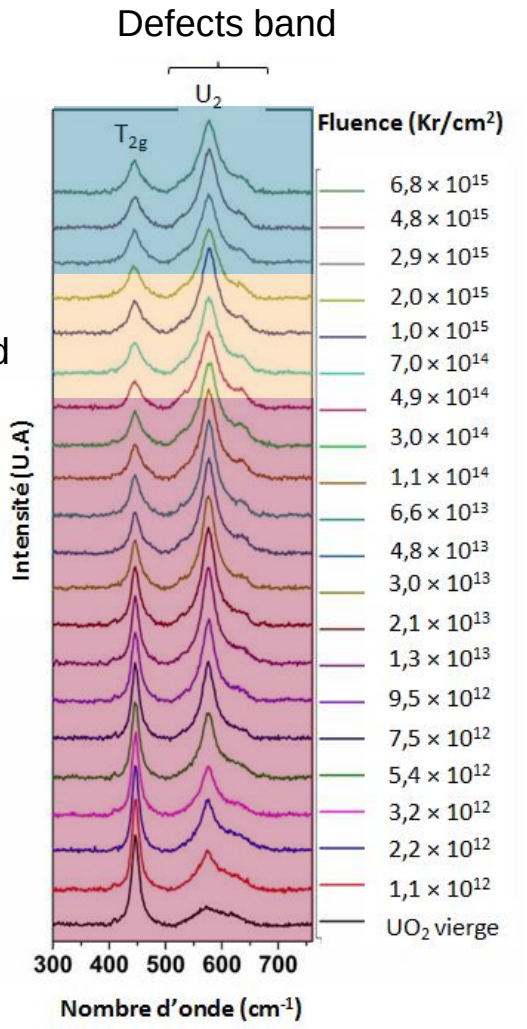

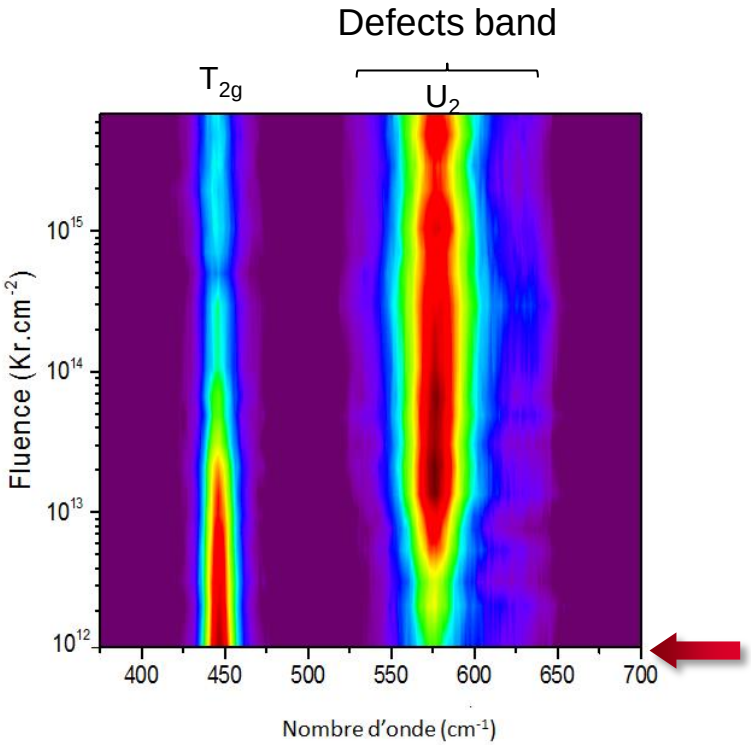

C. Onofri, C. Sabathier, H. Palancher et al., NIMB 374 (2016) 51

2. Evolution of extended defects in UO_2 under Xe irradiation

C. Onofri, C. Sabathier, S. Miro et al.

C. Onofri et al., EMIRUM2016, 20-21/10/16, Saclay, France

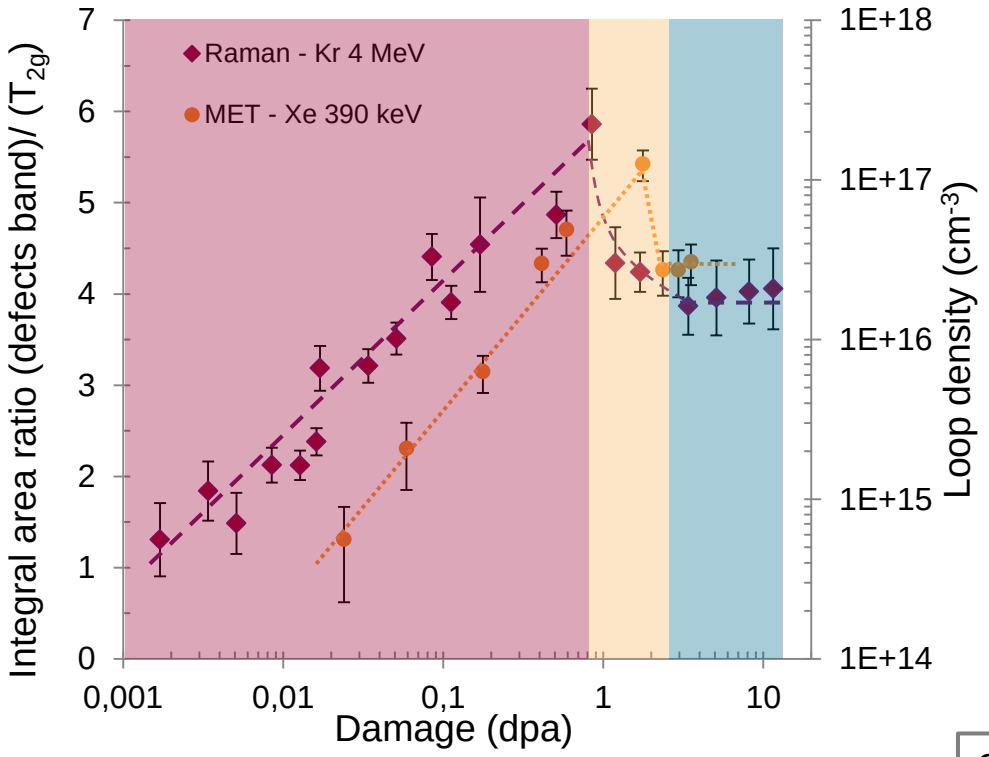

Small loops nucleation stage (< 10 nm)

Loops transformation into lines by overlapping

Steady state: lines and continuous nucleation of small loops (< 10 nm)

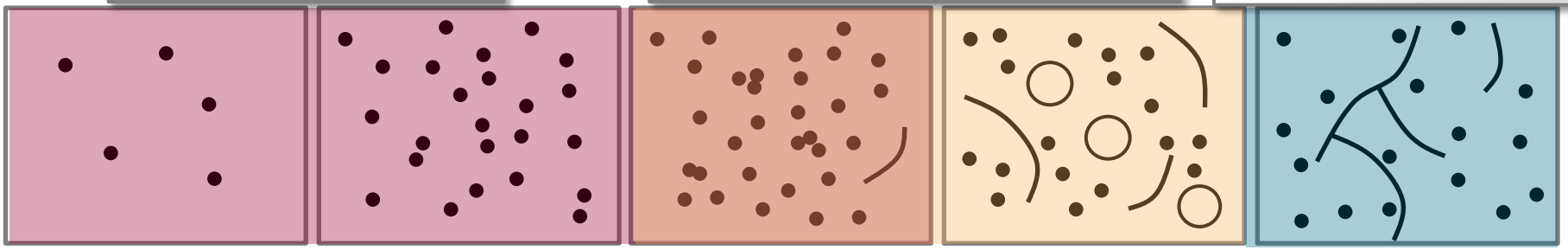

Role of irradiation in the oxidation of Zr-alloys

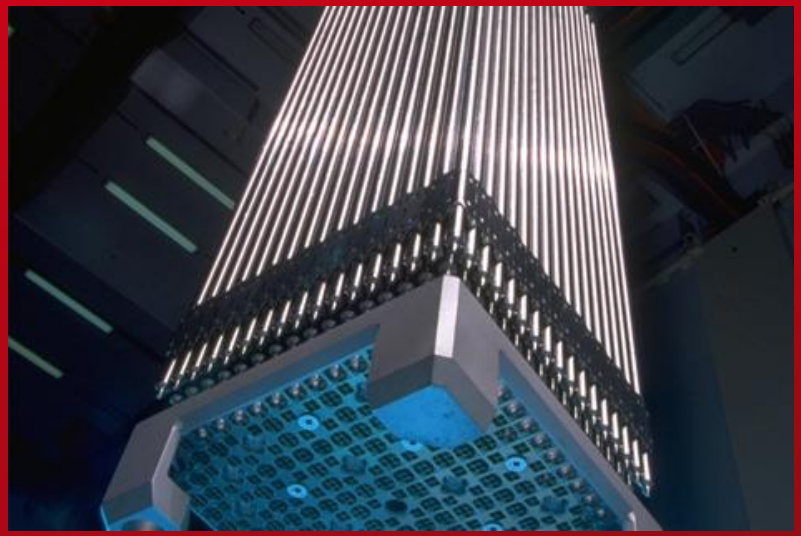

3. Oxidation of Zr alloys - background

- The fuel cladding in Pressurized Water Reactor

M. Tupin, S. Miro

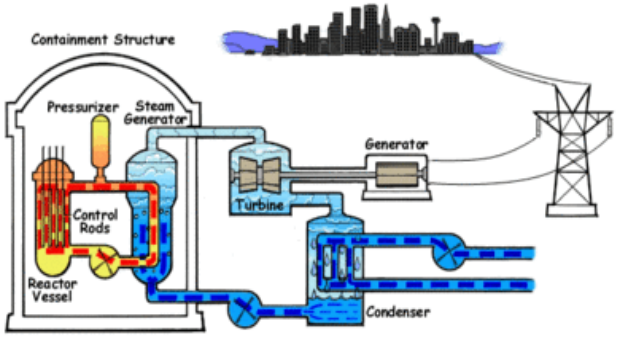

PWR

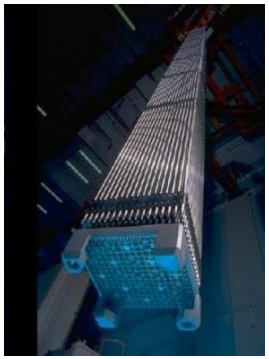

Fuel assembly

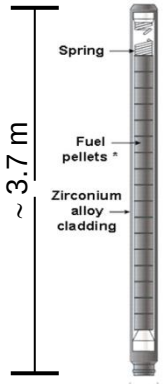

Fuel rod

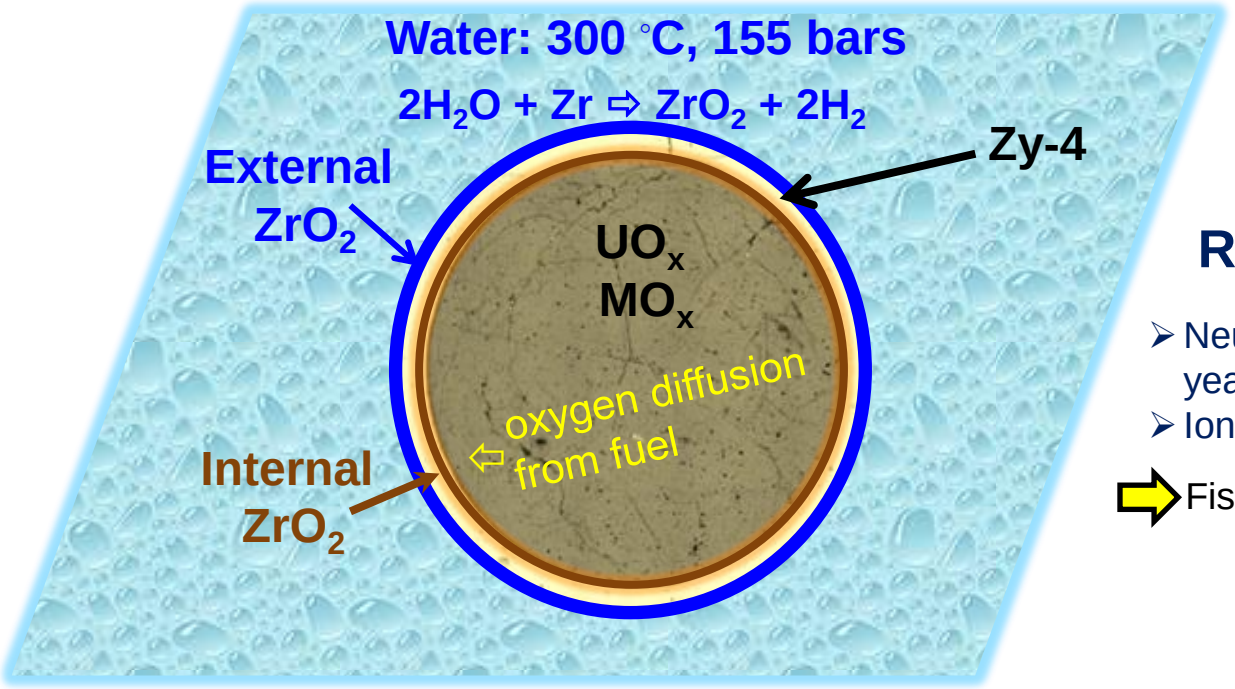

Radiation from

- Neutron displacement cascades ~3 dpa per year in the metal
- Ionization by X, γ and β-rays

⇨ Fission products for the internal oxide layer.

3. Accelerated oxidation of Zr alloys

M. Tupin, S. Miro

- Zr-alloys corrode in PWR primary water with formation of thick zirconia layer
- Oxidation rate of Zircaloy-4 cladding increases for burnups above 35 GWd/MtU
- The acceleration in oxidation rate is not reproduce in static autoclave or in corrosion loop

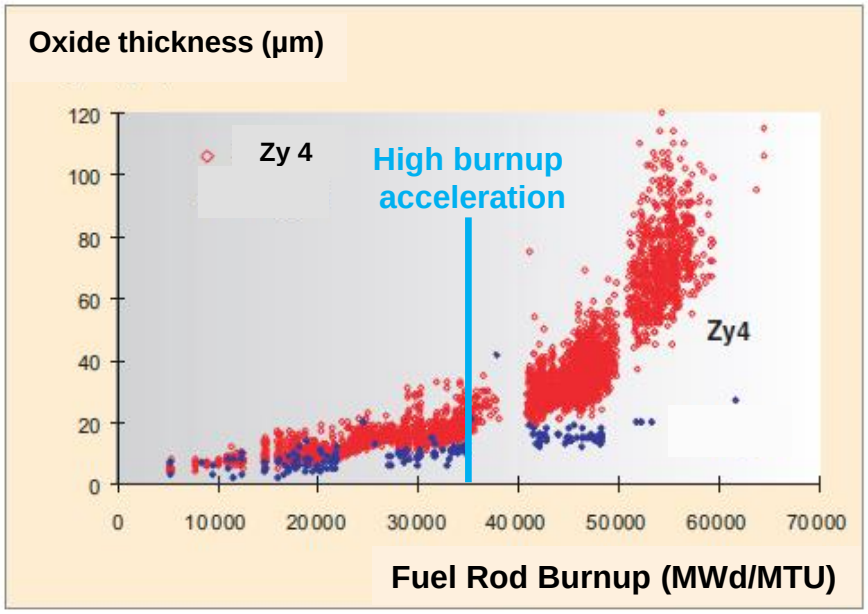

Corrosion performance of alloy M5 and Zr-4 fuel rods in PWR. A burnup of 35 corresponds approximatively to 3 years in reactor.

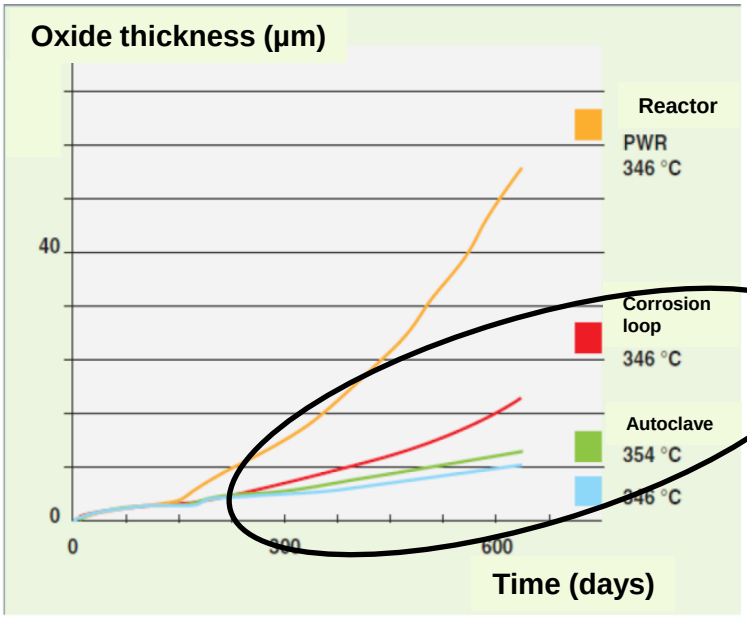

Oxidation rate of Zr-4 alloy , in autoclave (346 and 354 °C), PWR reactors and in corrosion -oops (with PWR hydrohydraulic conditions).

Hypothesis to be tested: radiation damage plays a role in the oxidation increase at high burnup

3. Experimental method
Role of irradiation in the oxidation process

M. Tupin and R. Verlet, S. Miro

- Zircaloy-4 was corroded in an autoclave mimicking PWR conditions

Liquid water with 2 wppm Li from LiOH and 1000 wppm B from H_3BO_4 at 360°C and 187 bars

→ After 40 days a 1.5 µm thick oxide layer is formed on the metal

Autoclave

- Irradiation of zirconia

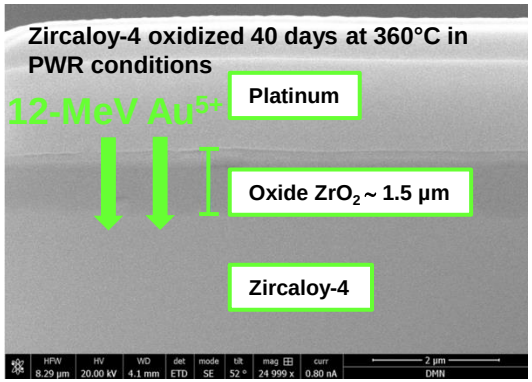

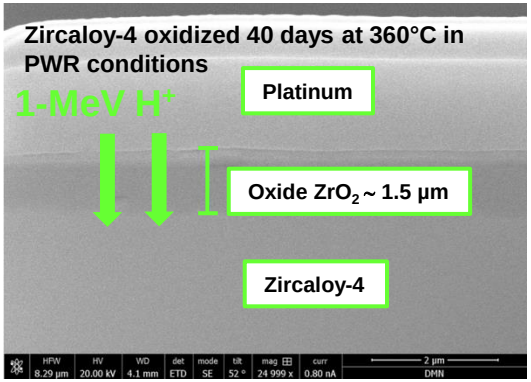

JANNUS

Japet, Au 12MeV
Epiméthée, H 1MeV

Ion	Energy	R_p	dpa (max)	S_e/S_n
Au^{5+}	12 MeV	1.6	13	0.7
H^+	1 MeV	9.2	0.03	2500

→

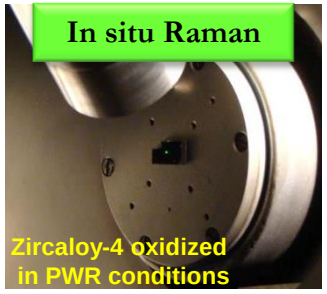

3. Ion-irradiation of pre-oxidized Zr-alloy with *in situ* Raman characterization

S. Miro et al. J. Raman Spectrosc. 2015

M. Tupin and R. Verlet, G. Gutierrez

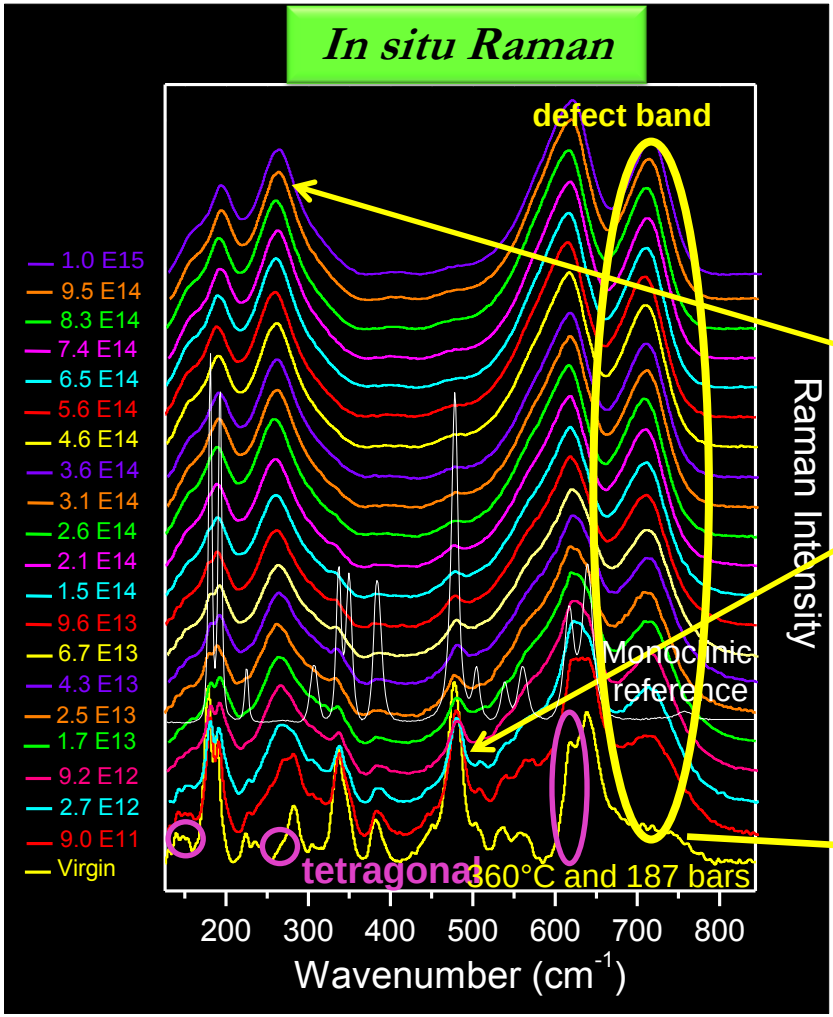

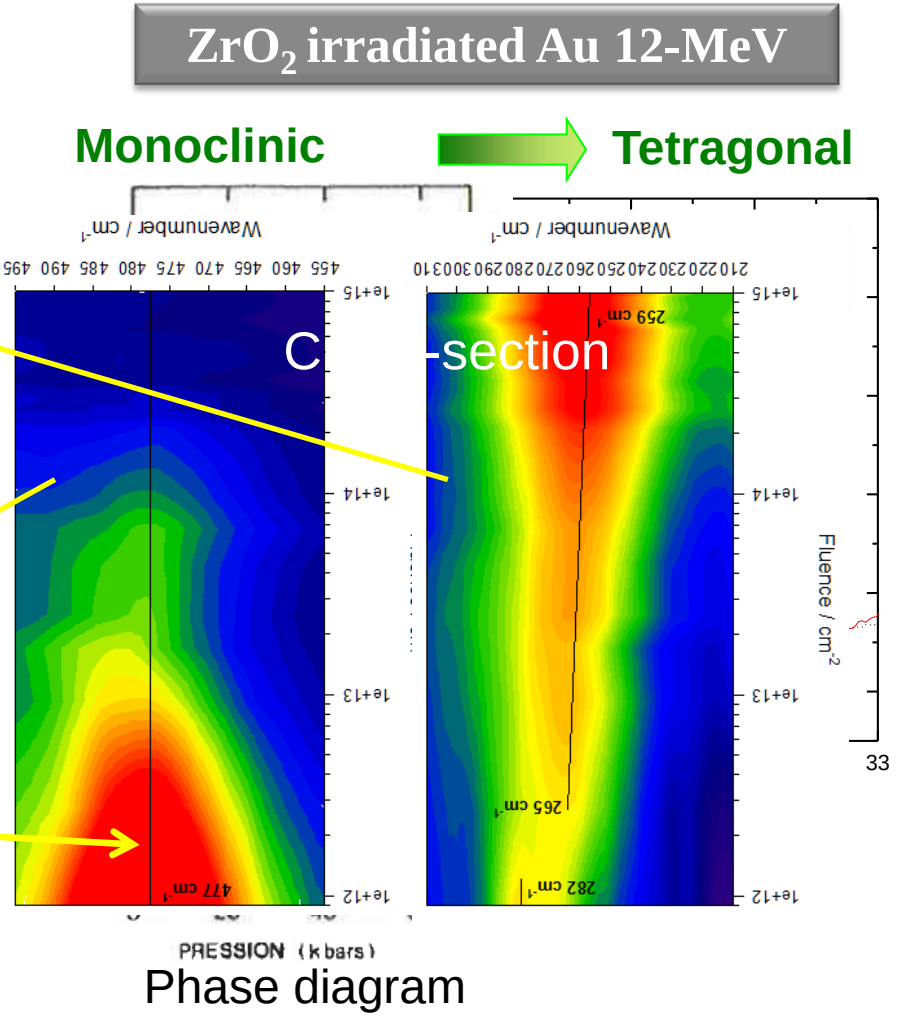

Phase diagram

Monoclinic phase transforms into tetragonal + specific band (defects)

3. Comparison of Zr-alloy from lab and from reactor

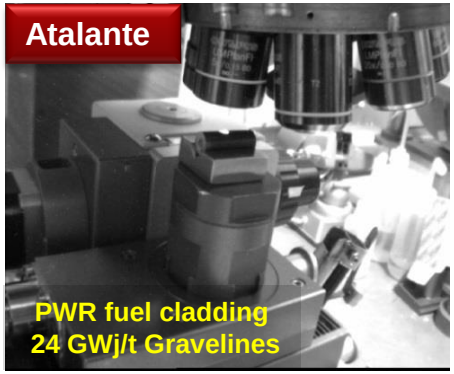

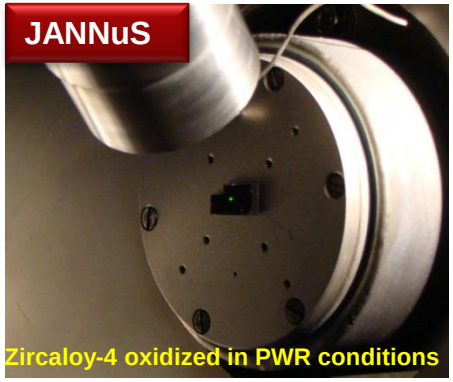

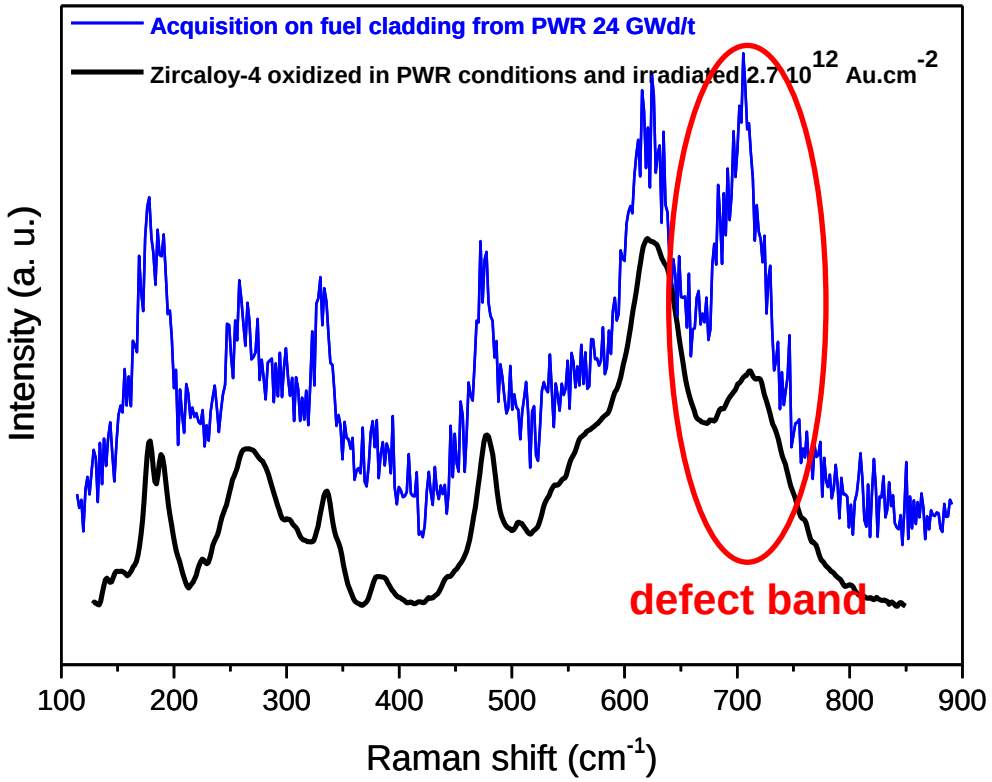

Equivalent Raman spectrum with a defect band

3. Irradiation of pre-oxidized Zr-alloy with *in situ* Raman characterization

- **12 MeV Au irradiation vs 1 MeV H irradiation**

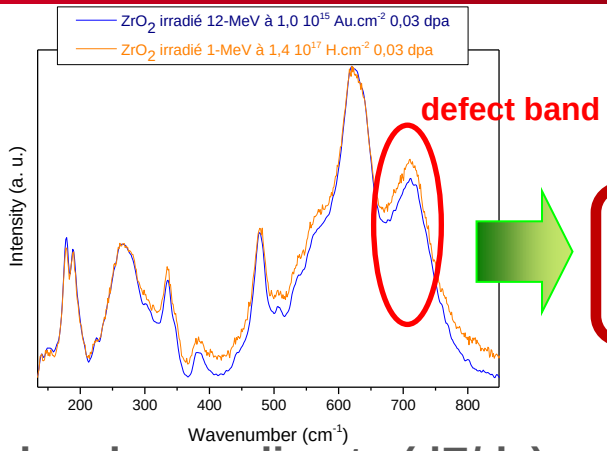

M. Tupin and R. Verlet, S. Miro

Different fluence and same dpa give equivalent Raman spectra.

- **Evolution of the defects band according to $(dE/dx)_e$ or $(dE/dx)_n$**

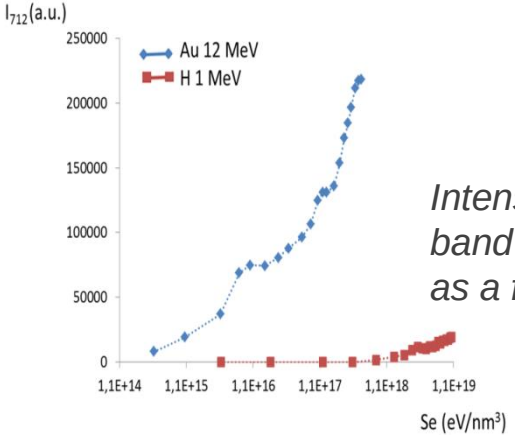

Intensity of the 712 cm^{-1} band in the oxide layer as a function of $(dE/dx)_e$.

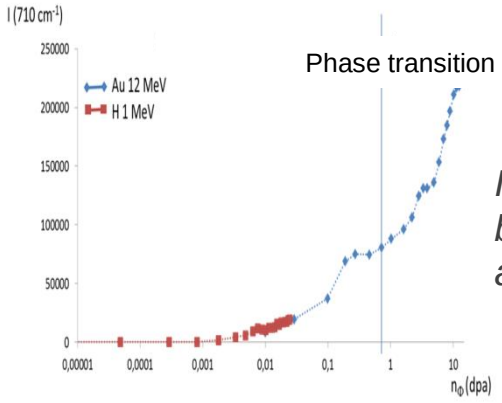

Intensity of the 712 cm^{-1} band in the oxide layer as a function of $(dE/dx)_n$.

Ballistic effects are responsible for irradiation damage
Raman spectrum signs a strong disorder in the oxygen sub-lattice of the tetragonal phase ⇒ defects are probably oxygen bi-vacancies [Vo, Vo˙]˚

J.-M. Costantini et al.JNM, 440(2013) 508-514.

3. Further oxidation of pre-corroded and pre-irradiated Zr-alloy

M. Tupin and R. Verlet, S. Miro

- **After a sequence of oxidation/irradiation, Zircaloy-4 was put back in an autoclave mimicking PWR conditions for further corrosion**

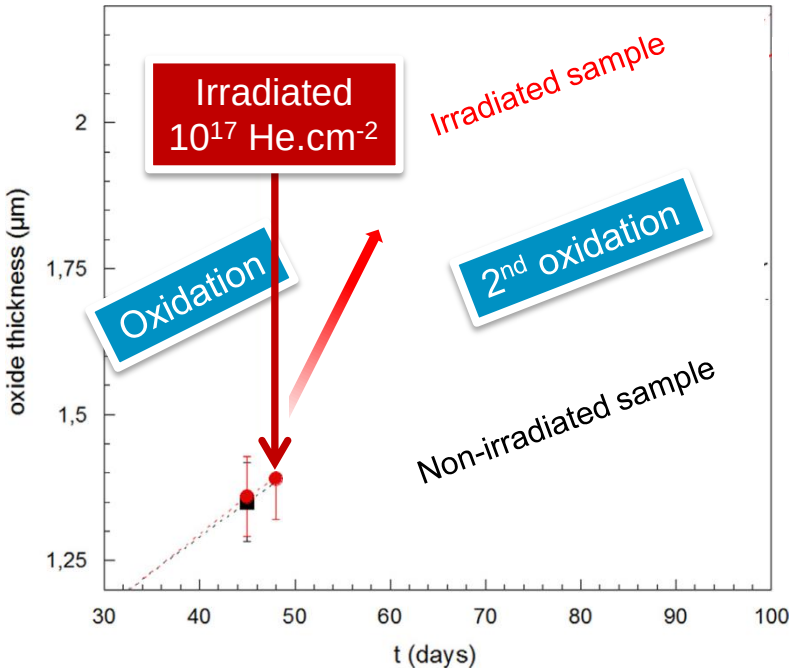

Evolution of oxide thickness on Zircalloy4 exposed in PWR conditions

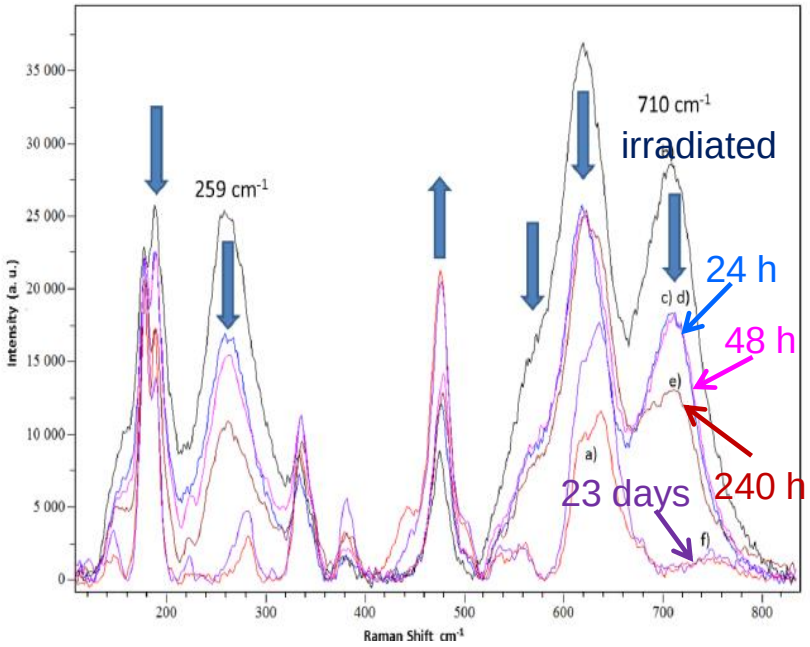

Raman spectra of the oxide layer irradiated with He 1.3MeV at 10^{17}.cm^{-2} and re-oxidized in PWR conditions

Irradiation (in the oxide) increases the oxidation rate
After a strong transient increase, irradiation defects thermally anneal and the oxidation rate is equivalent to that of a non-irradiated material.

R. Verlet, Corrosion Science 98, 327-338 (2015)

3. Analysis of external zirconia formed in reactor

M. Tupin and R. Verlet, S. Miro

External ZrO_2

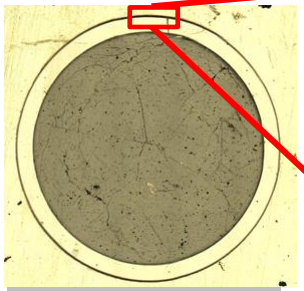

Rod cross-section

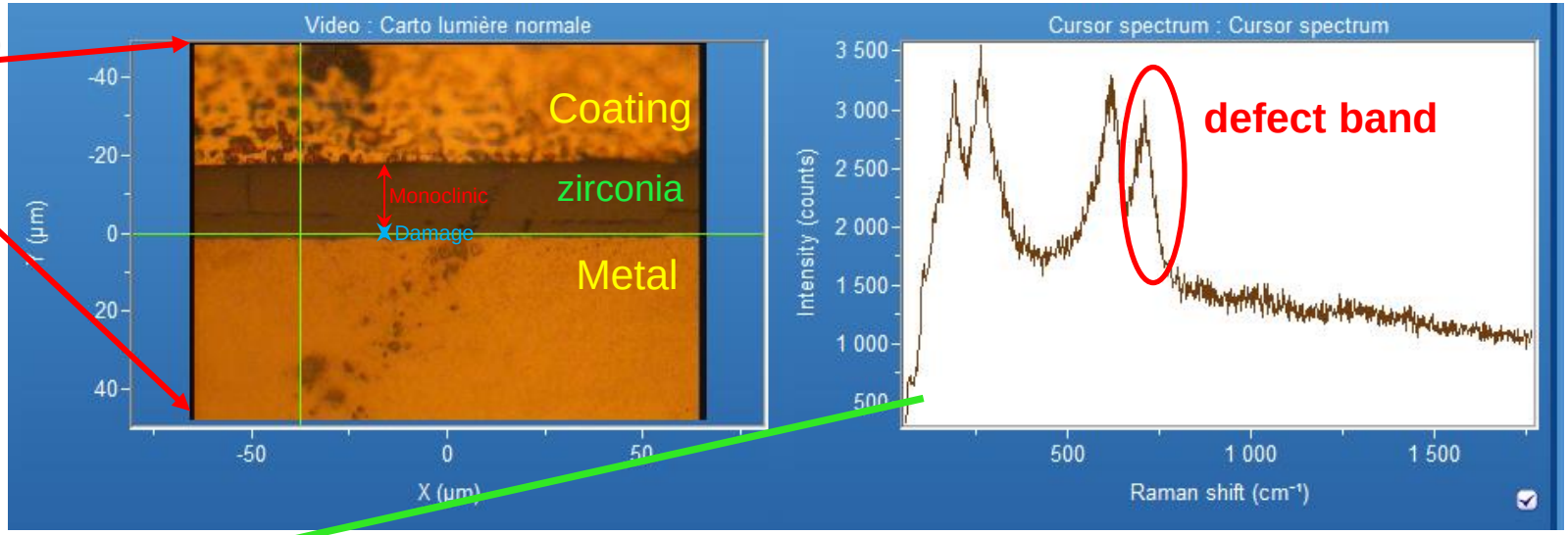

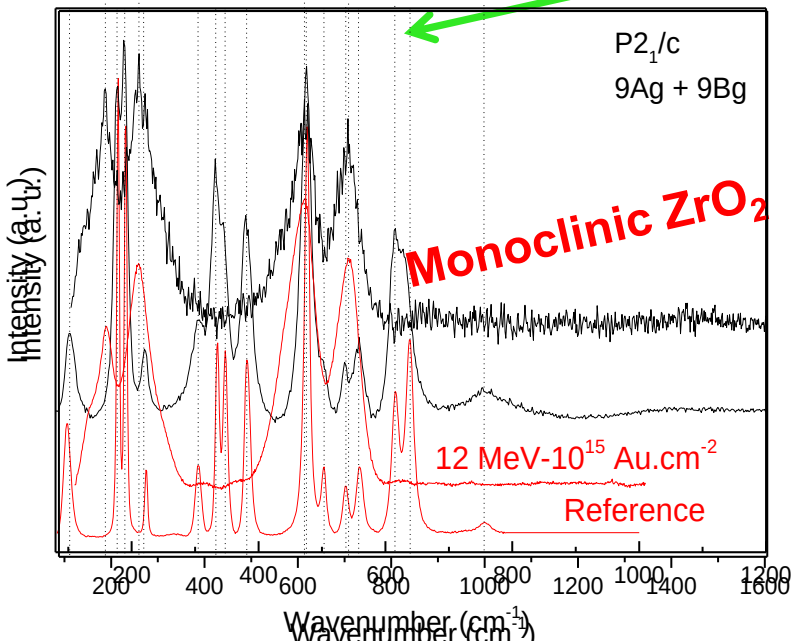

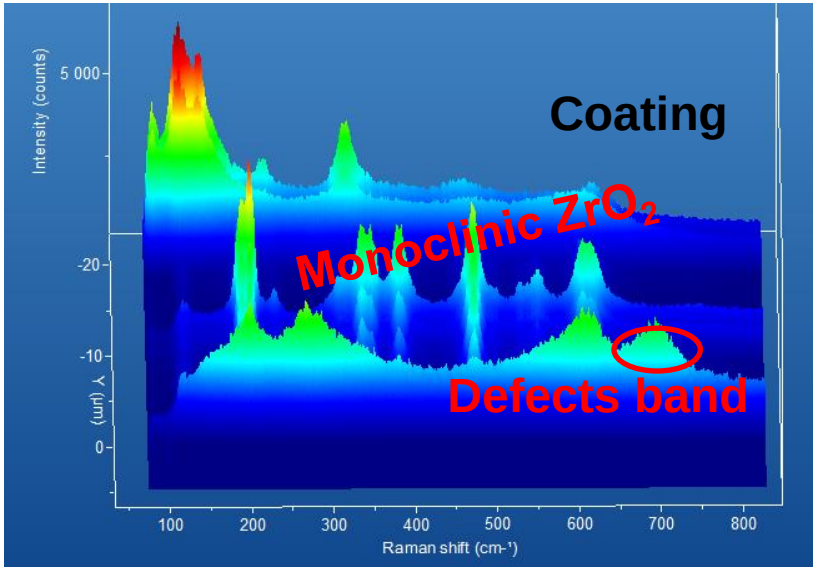

3. Analysis of internal zirconia formed in reactor

C. Ciszak, S. Miro

Internal ZrO_2

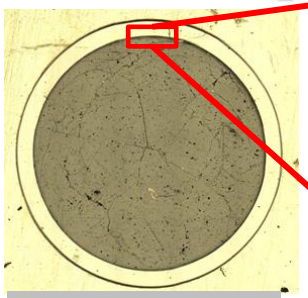

Rod cross-section

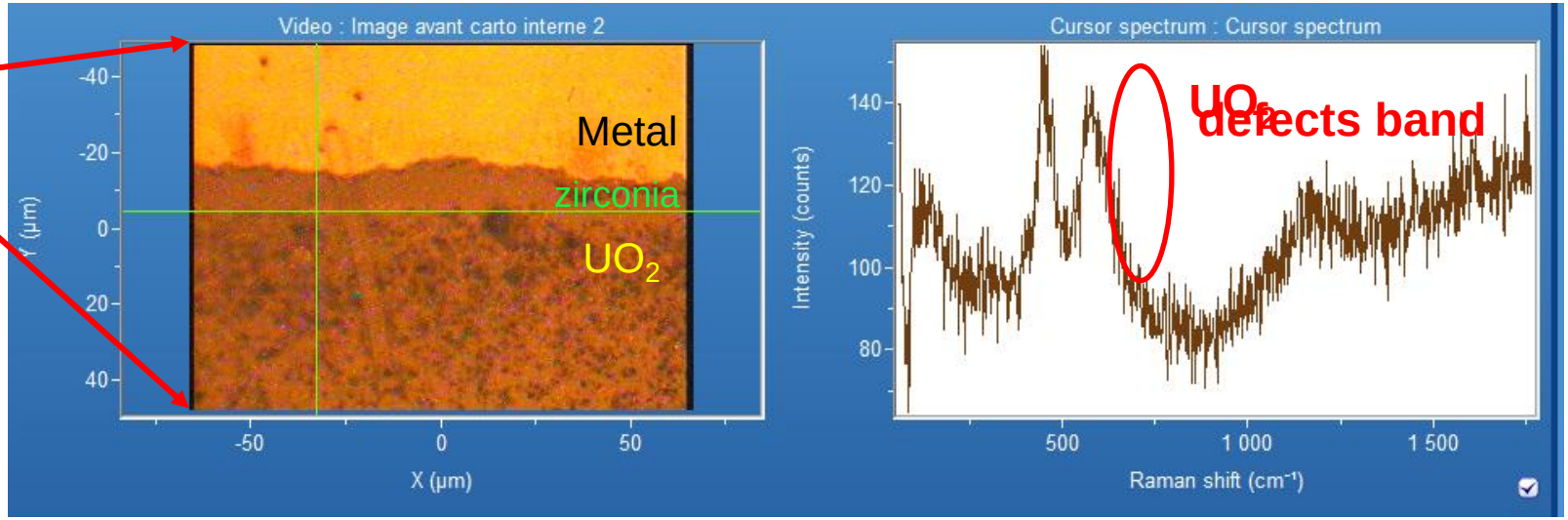

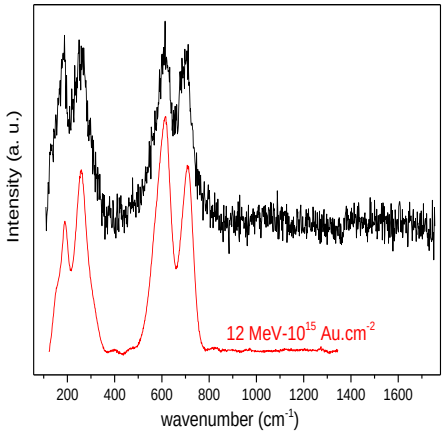

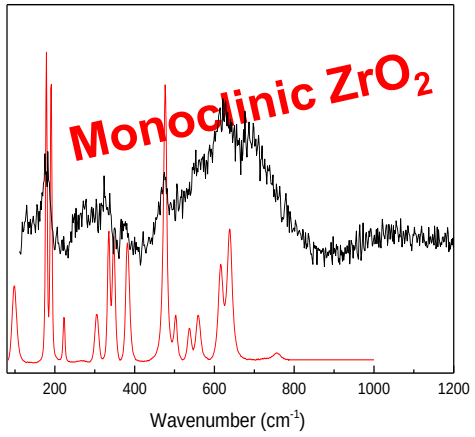

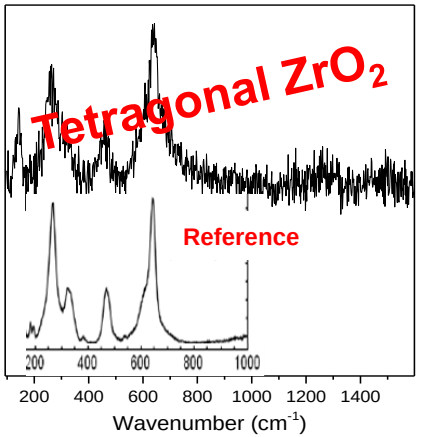

C. Ciszak et al. JNM

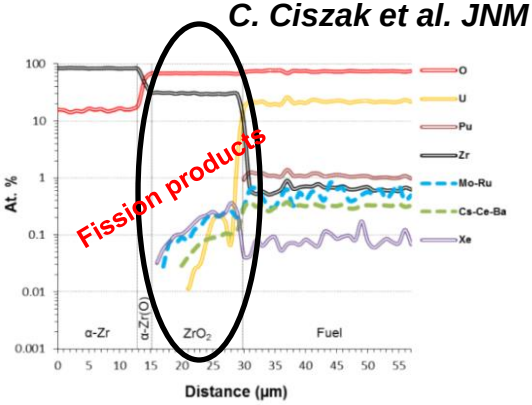

Electron Probe Micro Analysis

3. Role of radiation damage in the oxidation of Zr-alloys

S. Miro

External ZrO_2

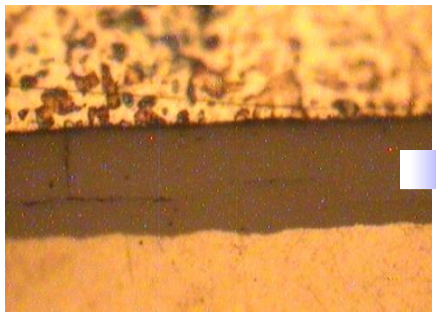

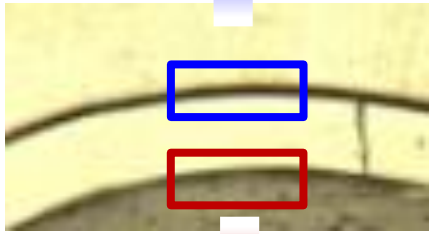

Internal ZrO_2

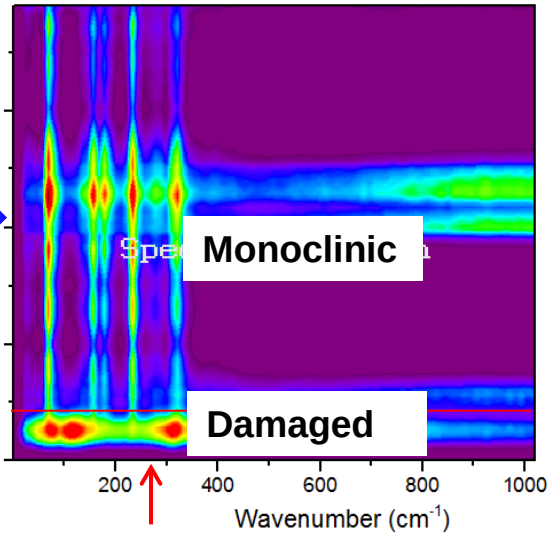

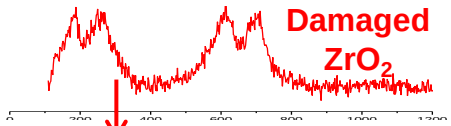

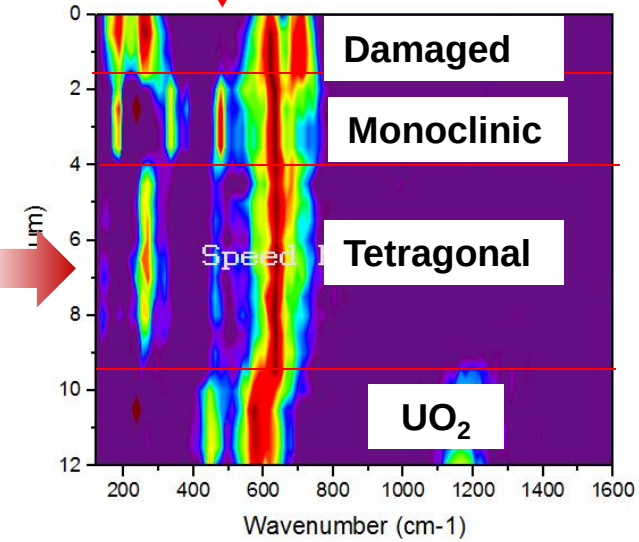

- Oxidation proceeds at the Zr/oxide interface
- Oxide is highly defective near the interface (oxygen vacancies)
- Radiation defects in the oxide increase the oxidation rate

Radiation defects seem to be a major contributor to the oxidation acceleration at high burnup

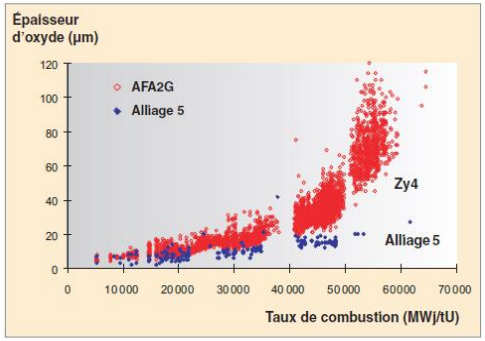

Precipitation in ferritic alloys
Dose rate effect

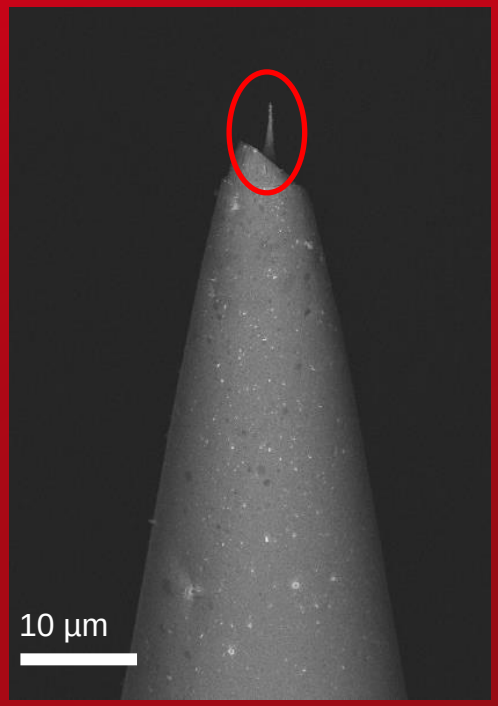

4. Data from irradiation campain in BR2

O. Tissot, C. Pareige, J. Henry, E. Meslin, B. Décamps

- **An irradiation program in BR2 and PIE were performed in the frame EU funded RD projects on binary Fe-Cr alloys with 5, 9% and 12% Cr**
  temperature ~300°C / max dose ~1.8 dpa / dose rate ~ 7 10^{-7} dpa/s
- **α' precipitate in Fe-12Cr [1-3], not in Fe-5Cr and Fe-9Cr (undersaturated)**
  ➔ radiation enhanced α' precipitation

➢ Estimated equilibrium composition of α phase at 300°C:

- SANS : 0.6 and 1 dpa : 8.8 ± 0.5 at.% [1]
- APT : 0.6 dpa : between 8.3 at.% and 8.8 at.% [2]
  1.82 dpa : 8.9 at.% [3]

➢ Composition of α' particles at 300°C:

- SANS : 0.6 dpa : 94 %Cr [1] (assumption)
- APT : 0.6 dpa : 58 ± 1 % Cr [2]
  1.8 dpa : 87 ± 4 % Cr [3]

→ solubility limit may have not been attained

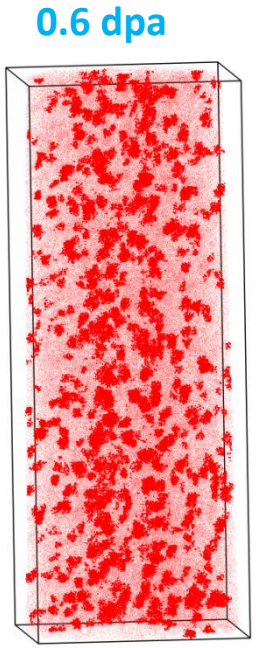

Fe-12%Cr – 300°C

[1] F. Bergner et al., Scripta Mater. 61 (2009) 1060, [2] V. Kuksenko et al., J. Nucl. Mater. 432 (2013) 160-165,
[3] M. Bachhav, et al. scripta 74, 48-51 (2014).

4. Self-ion irradiation of Fe-Cr alloys

O. Tissot, C. Pareige, J. Henry, E. Meslin, B. Décamps

Fe-15%Cr

Fe 2 MeV at 300°C

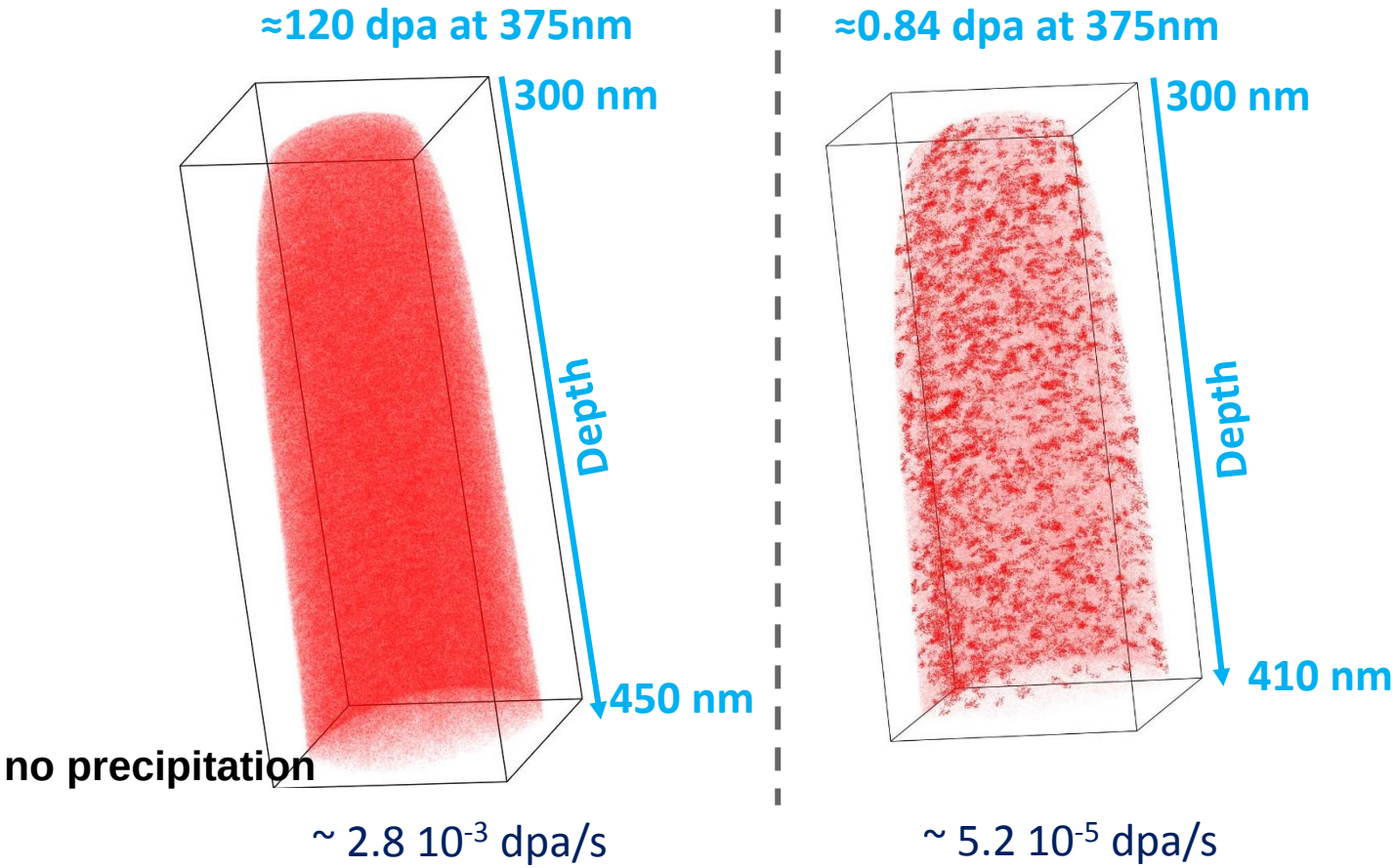

α' precipitation appears under self ion irradiation at low damage rates and low doses

4. Self-ion irradiation of Fe-Cr alloys at ‘low’ damage rate

Fe-15Cr, Fe 2 MeV, ~ 5.2 10^{-5} dpa/s, 300°C

O. Tissot, C. Pareige, J. Henry, E. Meslin, B. Décamps

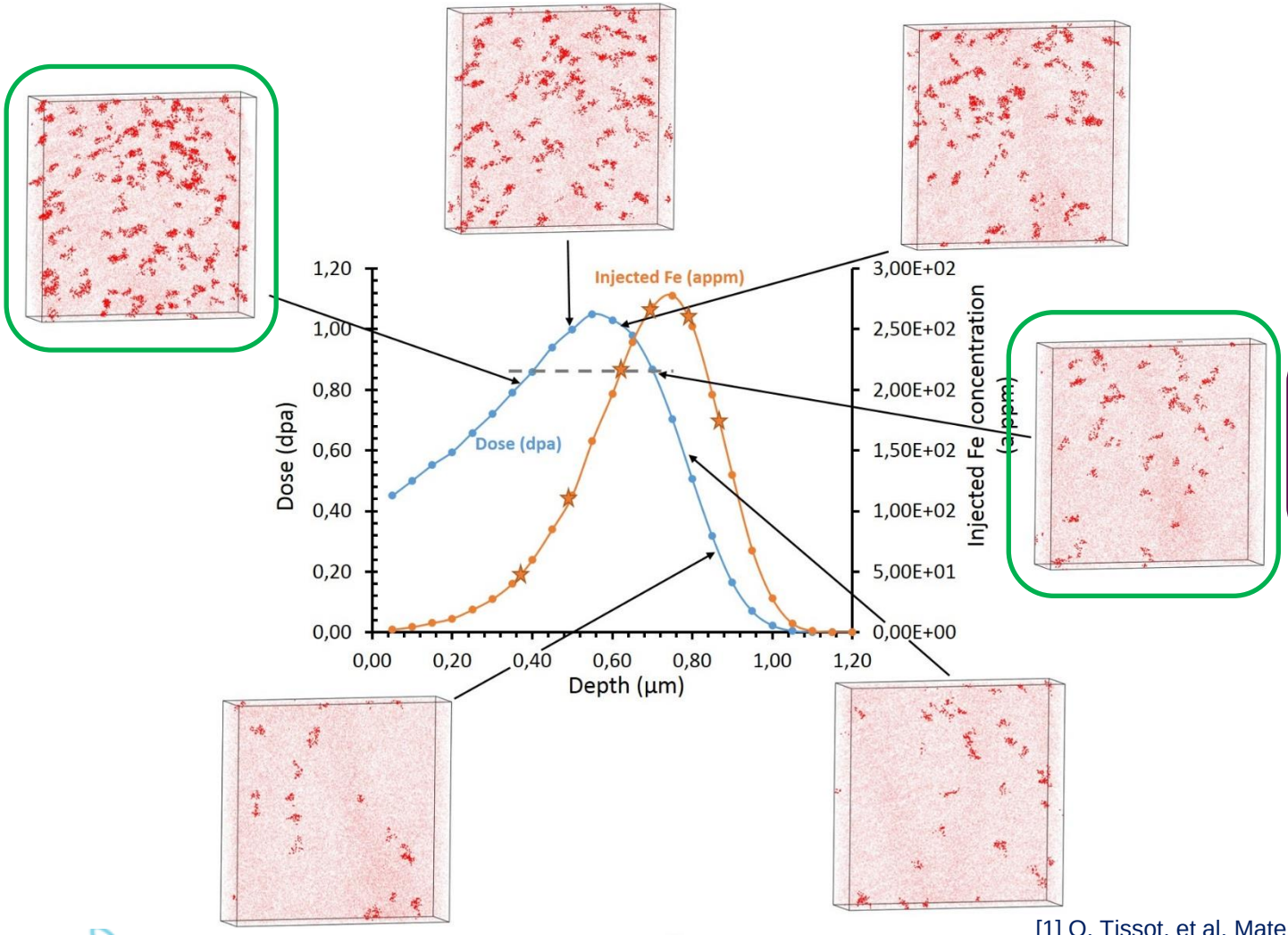

α' precipitation varies throughout the specimen

[1] O. Tissot, et al. Materials Research Letters

4. Self-ion irradiation of Fe-Cr alloys at 'low' damage rate

Fe-15Cr, Fe 2 MeV, ~ 5.2 10^{-5} dpa/s, 300°C

O. Tissot, C. Pareige, J. Henry, E. Meslin, B. Décamps

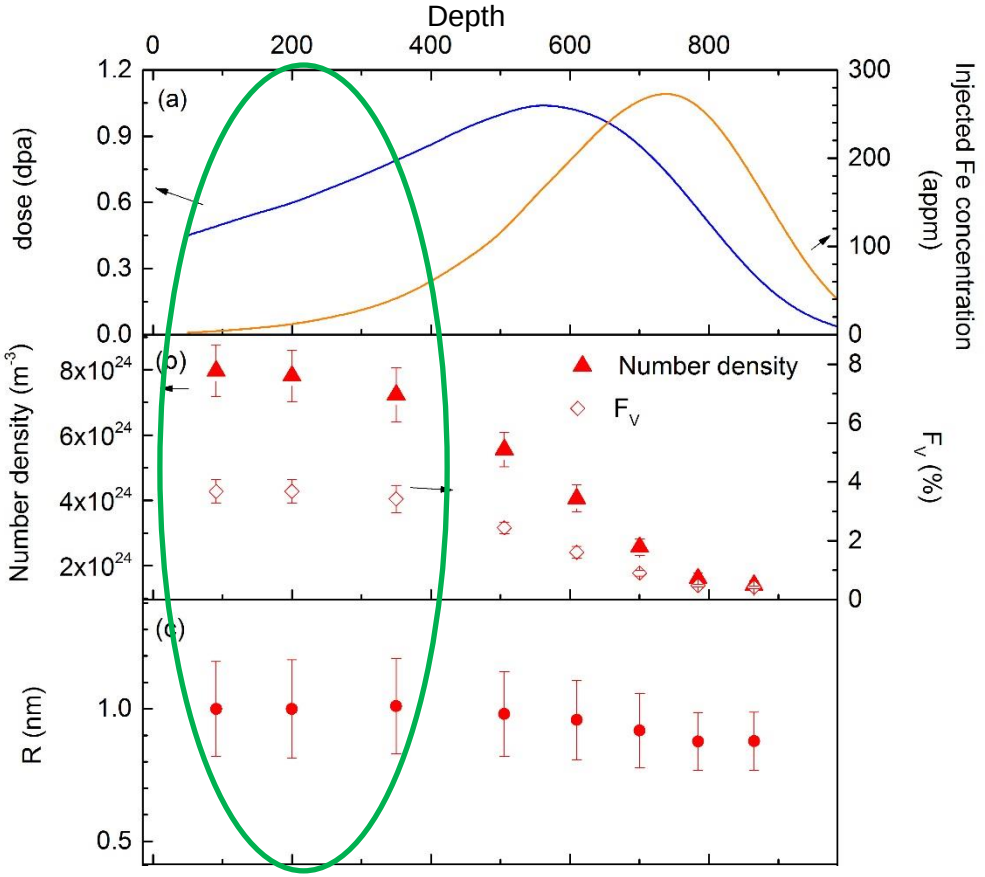

- 90 – 350 nm: dose increases but α' precipitation remains constant
- 350 – 900 nm: dose increases up to 550 nm, α' precipitation is reduced

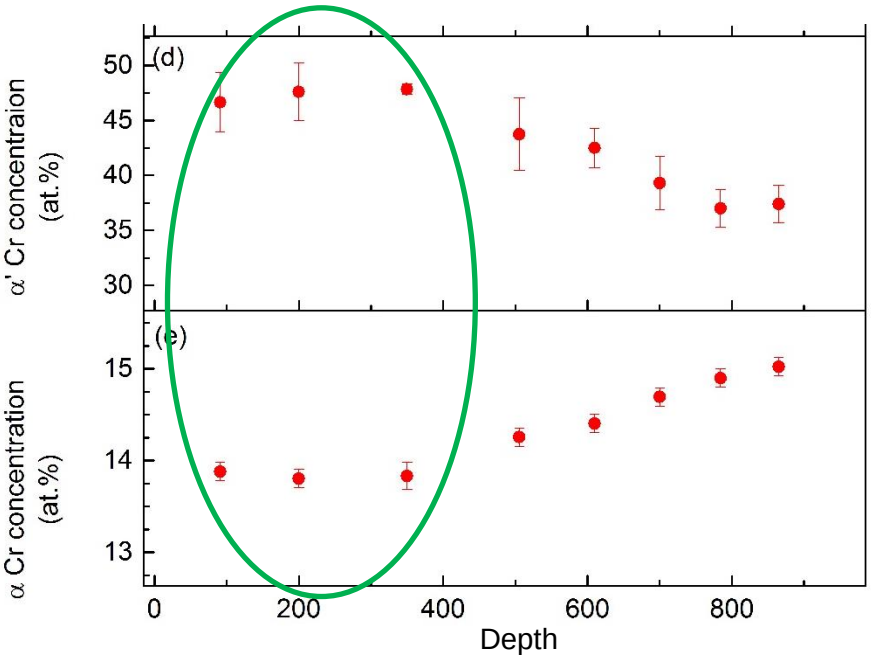

injected interstitials strongly reduce α' precipitation

[1] O. Tissot, et al. Materials Research Letters

4. Electron vs. self-ion irradiation of Fe-Cr alloys at 'low' damage rate

Fe-15Cr, ~ 4-5 10^{-5} dpa/s, 300°C

electrons (5h) [1]

0.7 dpa

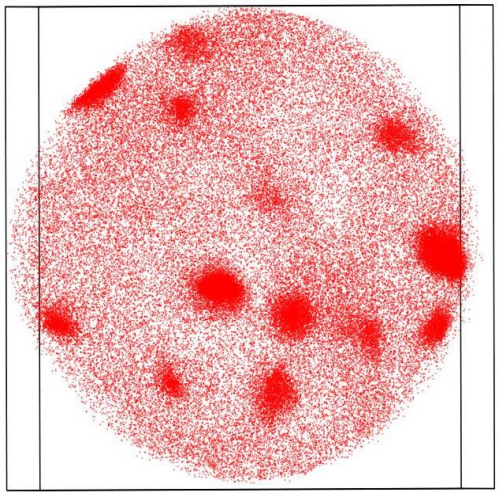

~ 4 10^{-5} dpa/s

Fe 2MeV (4.30 h)

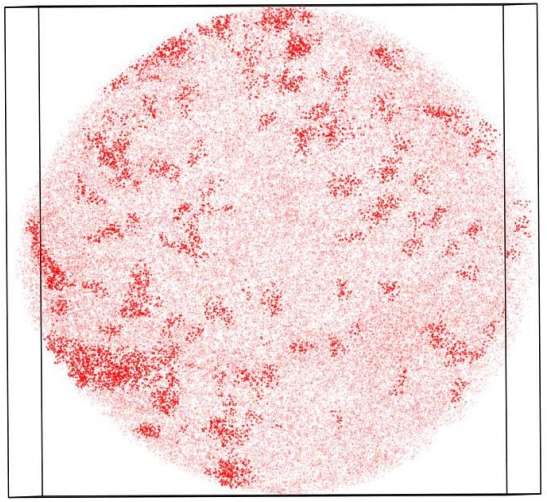

0.8 dpa

~ 5 10^{-5} dpa/s

- **α' much less developed after ion irradiation due to :**
  - **Difference in point defect creation**
  - **Injected interstitials**

[1] O. Tissot, et al. Scripta. Mater. 122 (2016) 31–35.

4. Self-ion irradiation of Fe-Cr alloys

O. Tissot, C. Pareige, J. Henry, E. Meslin, B. Décamps

Fe-15%Cr

Fe 2 MeV at 300°C

No α' precipitation under self ion irradiation at high damage rate and high dose

≈120 dpa at 375nm

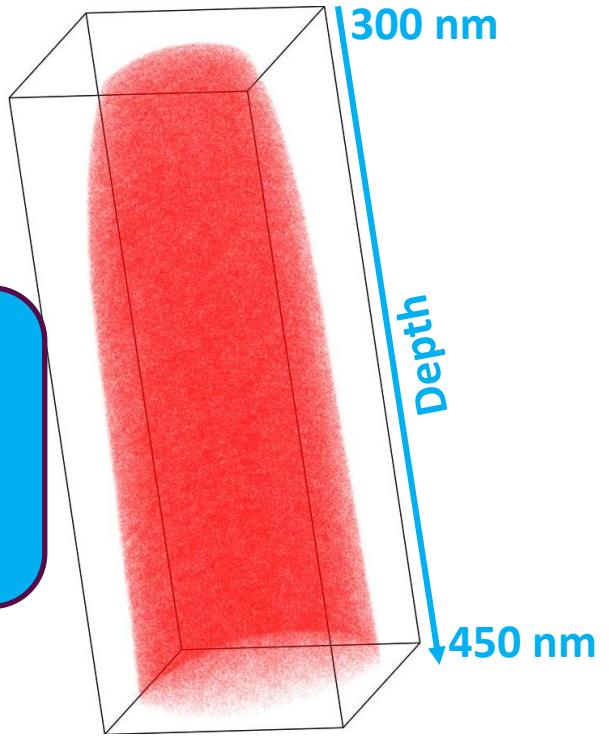

~ 2.8 10^{-3} dpa/s

≈0.84 dpa at 375nm

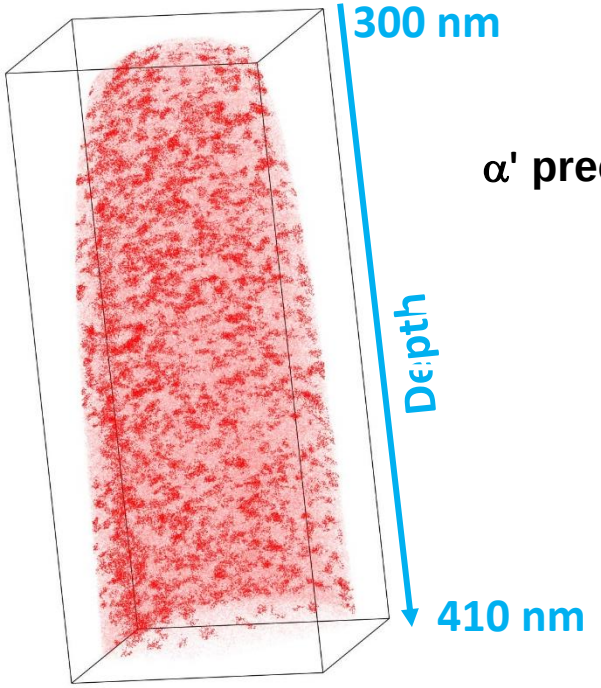

~ 5.2 10^{-5} dpa/s

α' precipitation

4. Dose rate effect

adapted from G. Was

Point defect balance equation

$$\frac{\partial C_v}{\partial t} = K_0 - K_{iv} C_i C_v - K_{vs} C_v C_s + \nabla \cdot D_v \nabla C_v$$

$$\frac{\partial C_i}{\partial t} = K_0 - K_{iv} C_i C_v - K_{is} C_i C_s + \nabla \cdot D_i \nabla C_i .$$

production

recombination

loss to sinks (voids, loops)

gradient

- ✓ production depends on dose rate
- ✓ recombination and sink strength are temperature dependent

Mansur assumed

- Defects absorption at sinks is the main contributor to microstructure changes:
  - Atomic diffusion for total i and v flux to sinks
  - Swelling for preferential v flux to sinks
- When dose rate increases, the production of defects increases and a lower dose is needed to keep the same number of defects to be absorbed at sinks. Alternatively for a given dose, temperature can be increased.

➢ Relationships from the invariance requirement for temperature / dose rate

[1] L.K. Mansur, JNM 206 (1993) 306-323

4. Dose rate effect

adapted from G. Was

Invariance requirements for temperature / dpa rate

Same point defect absorption at sinks relevant for RIS

$$T_2 - T_1 = \frac{\left(\frac{kT_1^2}{E_m^v}\right)\ln\left(\frac{\phi_2}{\phi_1}\right)}{1-\left(\frac{kT_1}{E_m^v}\right)\ln\left(\frac{\phi_2}{\phi_1}\right)}$$

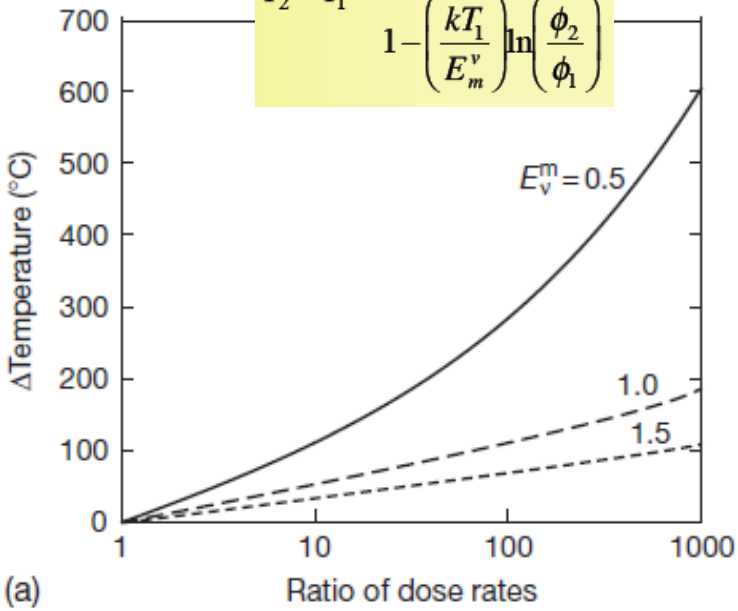

Swelling invariance

$$T_2 - T_1 = \frac{\left(\frac{kT_1^2}{E_m^v + 2E_f^v}\right)\ln\left(\frac{\phi_2}{\phi_1}\right)}{1-\left(\frac{kT_1}{E_m^v + 2E_f^v}\right)\ln\left(\frac{\phi_2}{\phi_1}\right)}$$

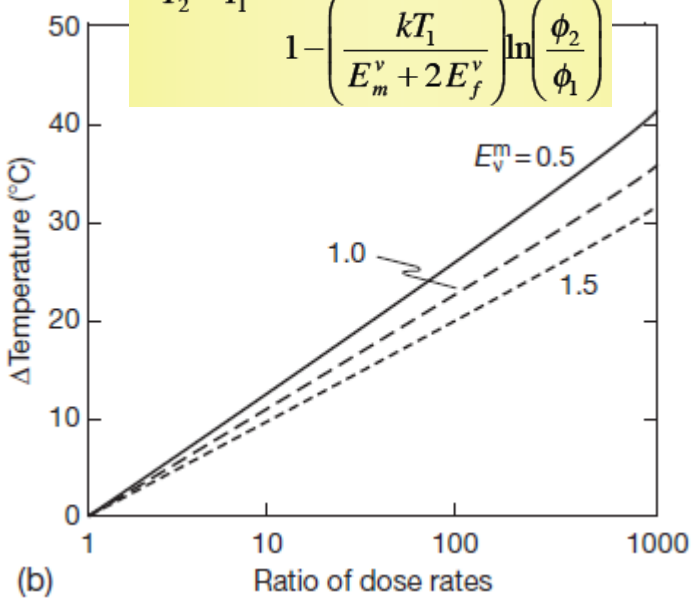

Temperature shift from the reference 200°C required at constant dose as a function of dose rate normalized to inital dose rate

E_{vm} vacancy migration energy **E_{vf} vacancy formation energy = 1.5eV**

[1] G.S. Was, Radiation Materials Science: Metals and Alloys, Springer, Berlin, 2007

4. Invariance requirement application to stainless steels

adapted from G. Was

Austenitic stainless steel neutron vs ion irradiation dose rate

	neutrons	protons	Ni^{2+}
Iso-adsorption of PD at sinks (RIS)	$\phi_n = 4.5\ 10^{-8}$ dpa/s $T_n = 275°C$	$\phi_p = 7\ 10^{-6}$ dpa/s T_p ~400°C	$\phi_{Ni} = 10^{-3}$ dpa/s T_{Ni} ~670°C
Swelling invariance	$\phi_n = 4.5\ 10^{-8}$ dpa/s $T_n = 275°C$	$\phi_p = 7\ 10^{-6}$ dpa/s T_p ~300°C	$\phi_{Ni} = 10^{-3}$ dpa/s T_{Ni} ~340°C

Evm=1.3eV, Evf=1.9eV

- **Temperature shift due to higher dose rate is dependent on the microstructure feature of interest**
- **A compromise is needed between extremes for same PD adsorption at sinks and swelling invariant**
- **With increasing diffrence in dose rate, the ΔT between low dose rate (neutron) and high dose rate (heavy ions) inceases**

4. Possible reasons for diffrences in α' precipitation

Fe-Cr alloys at 300°C

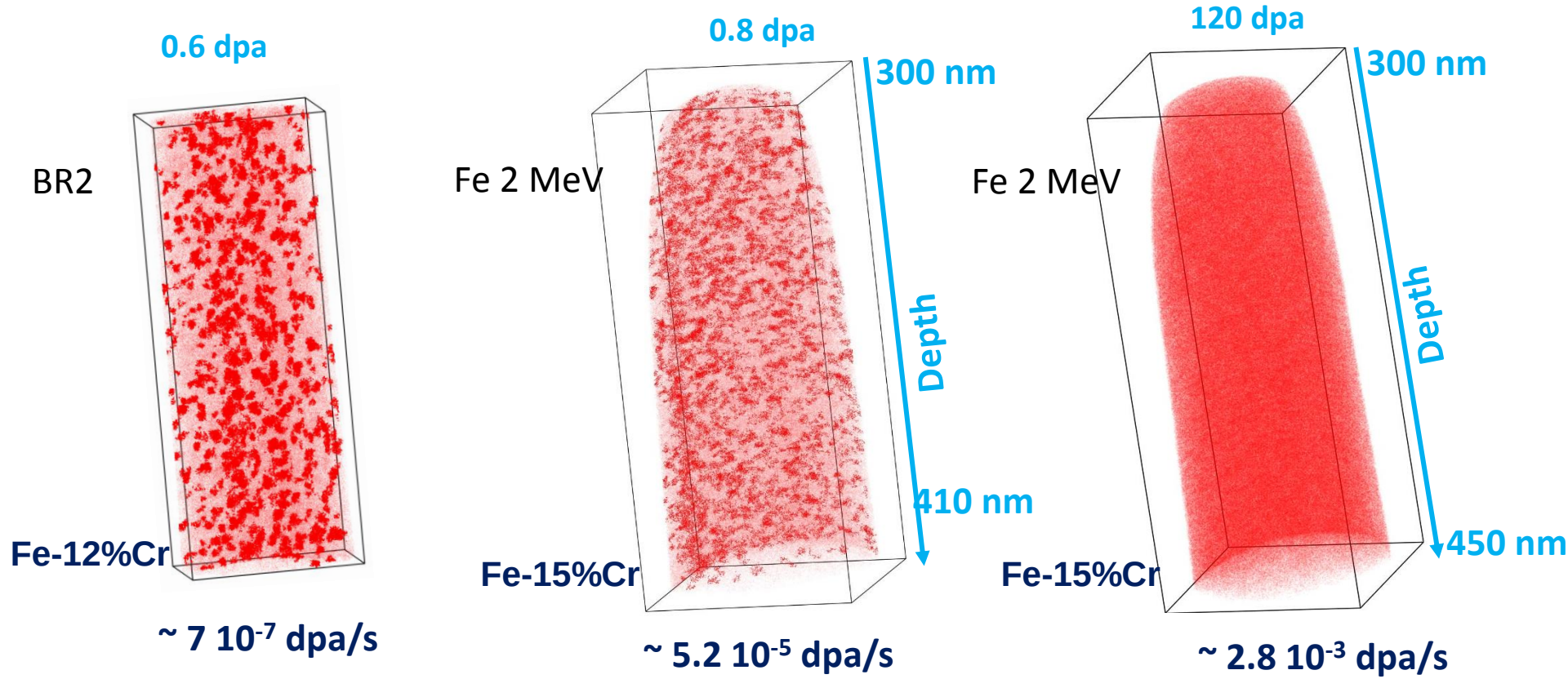

α' precipitation may be favored by low dose rate according to the microstructure invariance requirement

Success in matching neutron-irradiated microstructure: FFTF and Fe^{++}

HT9 heat 84425, ACO3 duct

from G. Was

Loops | G-phase in matrix | G-phase on G.B. | Voids

Fe^{++}, 460ºC
5×10^{-4} dpa/s
188dpa
1 appm He

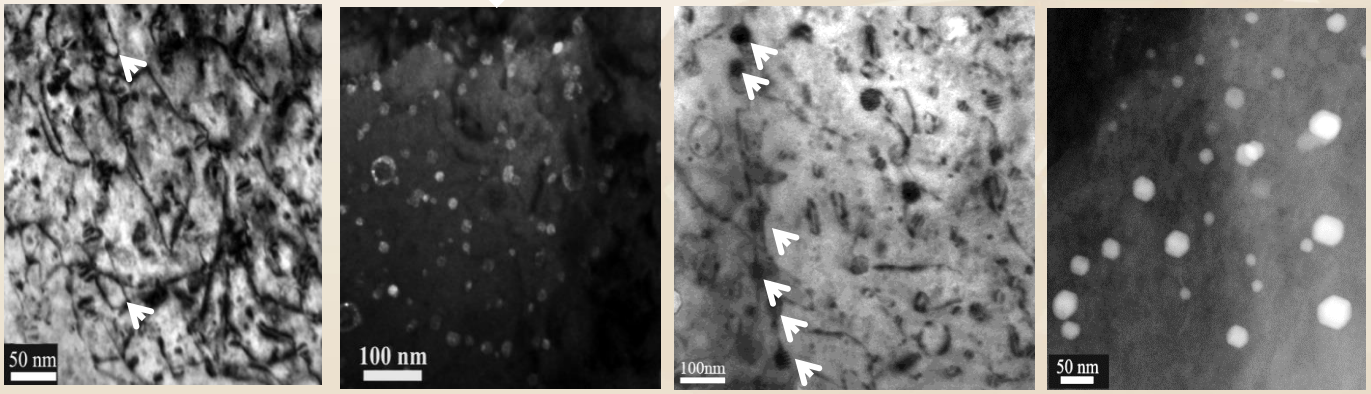

FFTF, 440ºC
7×10^{-7} dpa/s
155dpa

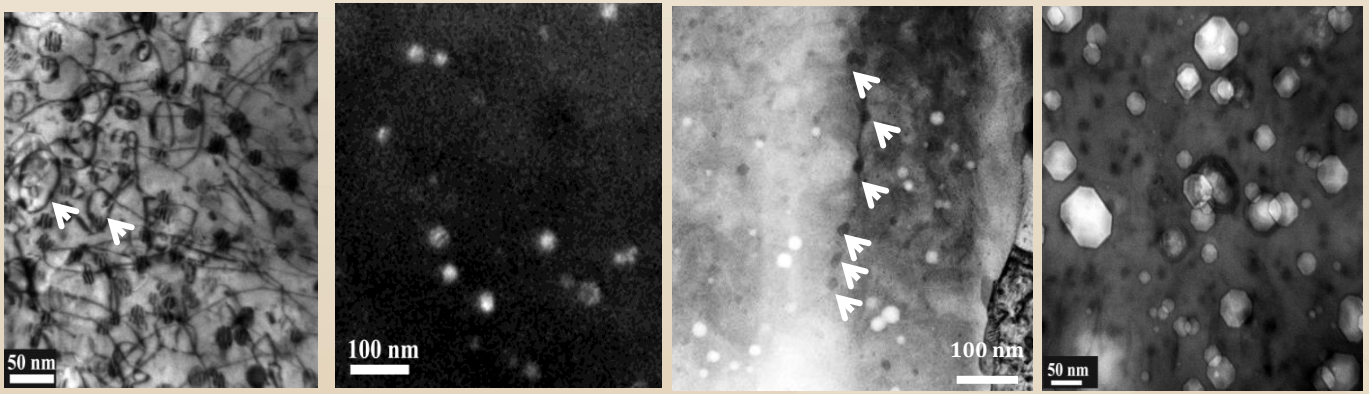

Conclusion: ion irradiation can add value to neutron irradiation and give access to the extreme of high dose

Variable	Ion Beams	Reasearch Reactors
Dose	up to 100s dpa	10-20 dpa max
Dose rate	100 - 1000× reactor rates	Few × reactor rates
Energy	Controlled by ion type (a few keV to ~ 100 MeV)	Neutron spectrum (up to 14 MeV)
Transmutants/fission products	Separable	Controlled by nuclear physics
Temperature	Better than ±10° C	Variable – 10s of ° C
Residual activity	Low to none	high
In-situ observation	TEM, RS, GC, etc.	Some T and displacement, generally PIE only
Unit mechanisms	Demonstrated	Challenging
Cost	Relatively low	Relatively high
Simultaneity (e.g., corrosion and straining)	Corrosion, SCC, creep, diffusion, etc.	Bulk materials, doable but difficult
Sample thickness	A few nm to ~100 µm	bulk

time – in-situ analysis – parameter control

dose rate effect – thin sample

➔**Analytical studies, to be associated to a modelling approach**

from Wayne King

Céline CABET
CEA Paris-Saclay, DEN/DANS/DMN/SRMP
Laboratoire JANNUS
91191 Gif Sur Yvette
celine.cabet@cea.fr
Tel : +33 672458311